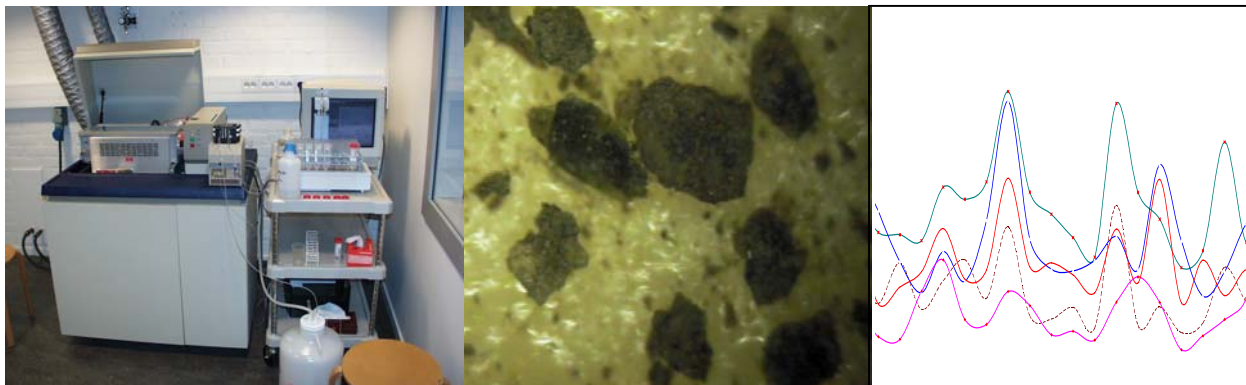


Speciation Analysis of Metals on Sediment Particles by Laser Ablation-Inductively Coupled Plasma-Mass Spectrometry (LA-ICP-MS)



Atindra Sapkota

Applied Environmental Measurement Techniques
(Master's Thesis)

Department of Water Environment Transport
CHALMERS UNIVERSITY OF TECHNOLOGY
Göteborg, Sweden 2002/12

Table of Contents

Abstract.....	Error! Bookmark not defined.
List of Figures	2
List of Tables	3
1 Introduction.....	4
1.1 Objectives	5
2 Importance of speciation in analytical chemistry	7
3 Limitations of Sequential Extraction	10
3.1 Lack of selectivity of reagents	10
3.2 Readsorption and redistribution.....	10
3.3 Sample pre-treatment.....	11
3.4 Methodology	11
4 Instrumentation of LA-ICP-MS.....	12
4.1 Principle of laser ablation system	12
4.1.1 Laser source	13
4.1.2 Optical devices.....	14
4.1.3 Sample cell and transportation system.....	14
4.2 ICP-MS for laser ablation	16
4.2.1 Instrumentation of ICP-MS.....	16
4.3 Limitations of LA-ICP-MS.....	18
5 Experimental methodology.....	20
5.1 Sampling and sample preparation.....	20
5.1.1 Sampling	20
5.1.2 Sample preparation	20
5.2 Instrument and operating conditions for analysis	21
6 Results and Discussions.....	23
6.1 Normalization of signals.....	23
6.2 Statistical analysis.....	24
6.2.1 Correlation results.....	26
6.2.2 Degree of association.....	31
6.2.3 Ternary plots and three-dimensional diagrams.....	33
7 Conclusion	35
Acknowledgement	36
References.....	37
Appendix I	41
Appendix II.....	45
Appendix III.....	51

List of Figures

Figure 1: Schematic diagram of the objectives of this study.....	6
Figure 2: Schematic diagram of the LA-ICP-MS system. Adapted from Durrant, 1999.	12
Figure 3: Energy level diagram for Nd: YAG laser. Adapted from Durrant, 1999.....	13
Figure 4: Schematic diagram of the arrangements of optical devices. Adapted from D. Gunther et al.....	14
Figure 5: Schematic diagram of the sampling cell and transportation port.	15
Figure 6: Schematic diagram of quadrupole ICP-MS. Adapted from Rauch, 2001.	18
Figure 7: Schematic diagram of sample preparation used for the ablation of sediment particles.	21
Figure 8: Picture of ICP-MS (left) and LA-ICP-MS (right) used at Chalmers University of Technology, Sweden.	21
Figure 9: A- Elemental profile of sediment particles before normalization. B- Normalized elemental profile of sediment particle.....	23
Figure 10: Elements showing different nature as observed for autocorrelation function vs. Lag-phase.....	25
Figure 11: Correlation or association coefficients between Pb and other elements.	27
Figure 12: Correlation or association coefficients between different elements.....	27
Figure 13: Mean correlation coefficient of Pb with other elements.	28
Figure 14: Diagram showing mean correlation coefficients and variability between different elements.....	29
Figure 15: Normalized profile of Si and S across the surface of a sediment particle.....	30
Figure 16: Normalized profile of different elements across the surface of a sediment particle.....	32
Figure 17: Figures showing the relationships between Pb/Mn/Fe and Pb/Mn/Mg	33
Figure 18: Three-dimensional relationship for the signal intensities between Fe, Mg and Pb.	33
Figure 19: Elemental profiles of different element on different particles used on this analytical work.....	41
Figure 20: Three-dimensional diagram showing the relationship between Fe, Pb and Mg.	51

List of Tables

Table 1: LA-ICP-MS operating parameters used for ablation of sediment particles	22
Table 2: Degree of association of Pb to different elements like Fe, Mn and Ca expressed as the percentage of association of elemental peaks	31
Table 3: Correlation between Pb-Mn and Pb-Fe	45
Table 4: Correlation between Pb-Cu and Pb-Zn.....	45
Table 5: Correlation between Pb-Cd and Pb-Mg.....	46
Table 6: Correlation between Pb-Ca and Pb-S	46
Table 7: Correlation between Pb-Si and Pb-K.....	47
Table 8: Correlation between Ca-S and Fe-S	47
Table 9: Correlation between Fe-Ca and Fe-Mg	48
Table 10: Correlation between Mg-Mn and Si-Fe.....	48
Table 11: Correlation between Si-Mn and Si-Mg.....	49
Table 12: Correlation between Si-Zn and Si-Cd.....	49
Table 13: Correlation between Si-S and Si-Ca.....	50
Table 14: Correlation between Si-K and Si-Cu	50

1 Introduction

Pollutants released in the environment through point and non-point source are mobilised, remobilised and acted on by physical, chemical and biological processes. Most of the pollutants find their way to the terrestrial and aquatic environments influenced by the depositional environmental conditions. Regarding this, aquatic systems are considered as the important sink for trace and bulk elements especially due to the industrial and traffic activities [Rice, 1999; Webb et al., 2000; Li et al. 2001]. This may be the reason that most of the environmental samples studied are from aquatic environment, especially when elemental speciation is considered [Das et al., 2001]. Some of the human activities and sources responsible for the release of metals include: agriculture (As, Cu, Hg, Pb, Se, and Zn); electrical power (As, Cd, Cr, Cu, Hg, Pb, Ni, Se, and Zn); metallurgy (As, Cd, Cr, Cu, Hg, Pb, Ni, and Zn); wood and pulp (As, Cd, Cr, Cu, Hg, and Pb) [Rice, 1999;].

Mobilisation of the trace and bulk elements in the aquatic systems/sediments is affected by the organic and inorganic particles like humics, polysaccharides, microorganisms, iron/manganese oxides and oxyhydroxides, and clays. The presence of these elements is dependent of the oxic and anoxic conditions prevailing on the system [Kiratli and Ergin, 1996; Webb et al., 2000; Bilali et al. 2002]. Moreover, trace and bulk elements in the sediments has been divided into different groups based on the binding fractions: exchangeable, bound to carbonates, bound to Mn-oxides, bound to Fe-oxides, bound to organic matter, bound to sulphides, bound to silicate and residuals [Tessier et al., 1979; Guo et al., 1997; Yu et al., 2001]. However, many studies of environmental samples on trace and bulk elements were limited to the determination of the total concentration of elements which was not considered as sufficiently informative about bioavailability, potential toxicity, and other physical-chemical behaviour [Tessier et al., 1979; Mester et al., 1998; Kot and Namiesnik, 2000], as these are dependent qualitatively and quantitatively on the binding properties of metals to the sediments [Yu et al., 2001]. To know about the above-mentioned characteristics of elements, study of elemental speciation is important [Tessier et al., 1979; Das et al., 2001]. Elemental speciation is the study of elements about the partitioning among the various form of elements, its adsorption strength with itself, other elements, organic and inorganic compounds. It has been further mentioned that speciation study is also useful for identifying the metals with a lithogenic origin from those of anthropogenic origin [Izquierdo et al., 1997].

The most widely used analytical technique for the elemental speciation in solid environmental samples e.g. sediments and soils are sequential extraction techniques. It is the study of speciation or fractionation or partition of elements in the sediments performed through selective leaching of elements from samples stepwise using different reagents or extractants [Mester et al., 1998; Rauch and Morrison, 2003]; therefore described as “operationally defined speciation” rather than true speciation [Mester et al., 1998].

Changes have been observed on the several procedures following the Tessier procedure of sequential extraction and thus given rise to many types of extraction procedures based

on different sequence of extractants and operating conditions [Mester et al., 1998]. This analytical procedure could be informative on the potential for release of trace elements from sediments under defined conditions rather than on true associations of trace and bulk elements with geochemical phase [Rauch and Morrison, 2003]. Furthermore, various extraction procedures and the lack of reference materials have attracted scientists to develop an analytical technique, which could enhance the accuracy and homogeneity of analysis all over the world [Mester et al., 1998]. Moreover, it is also a necessity of analytical technique where the solid samples could be used efficiently. Since many real/original environmental samples are of solid types, which often require cumbersome digestion procedure before analysis, direct analysis of samples on its original condition has been a long-term goal of analytical methods [Gunther et al., 1999]. It has been accepted that the study of elemental speciation should be efficient on development of highly sensitive analytical techniques that could function at ambient levels and small spatial scales [Rauch and Morrison, 2003] fulfilling the dream of analytical and process chemist where solid samples could be used directly [Gunther et al., 1999].

Advancement in laser ablation inductively coupled plasma mass spectroscopy has made it a widely accepted method for the analysis of solid samples for over decade [Alexander et al., 1998] and has enabled the study of elemental speciation or associations at micrometric scale providing sufficient resolutions for the investigation of elemental associations in sediments [Rauch and Morrison, 2003]. The analytical technique of LA-ICP-MS was investigated to acquire a complete elemental profile, specifically at trace and ultra-trace element levels [Walting et al., 1997]. Moreover, the advantages of using lasers for analysis of solids include little or no sample preparation, resulting in high sample throughput, application to almost all material and high spatial resolution allowing analysis of small selected areas [Arrowsmith, 1987]. Last few years have seen the application of LA-ICP-MS on the study of solid samples on various field of elemental speciation including: forensic science and purity of diamond [Walting et al., 1995; Walting et al., 1997], fingerprinting the components of road sediments [Rauch et al., 2000], association of platinum group metals with cerium [Rauch et al., 2000] and association of trace elements on sediment particles from urban river sediments [Rauch and Morrison, 2003].

1.1 Objectives

The objectives of this study or master's thesis are as follows (Figure 1):

- I. To gain a better understanding of elemental speciation and their importance in environmental science. This will be achieved through the reading of different articles related to elemental speciation. This will be discussed in brief in Chapter 2 "The Importance of elemental speciation".
- II. To understand and use relatively new instrumental analytical technique called Laser Ablation-Inductively Coupled Plasma-Mass Spectrometry (LA-ICP-MS).

Most of the elemental speciation carried out before are based on the sequential extraction technique. There will be a chapter 3 “Criticism of Sequential Extraction Technique” to know why LA-ICP-MS is useful instead of Sequential extraction technique. This chapter tries to describe some drawbacks of widely used analytical technique in the speciation analysis.

- III. As said in previous point about the LA-ICP-MS there will be a brief explanation about LA-ICP-MS in chapter 4, which provides the instrumental background. This background is considered to be useful for operating the instrument as well as act as a strong background for further study in the analytical study where this instrument is applicable. Sampling and sample preparation technique enhanced the knowledge for further study.
- IV. To know about the association of elements on the sediment particles. The analysis procedure for this study is classified as normalization of signals and statistical analysis of dataset. Under the normalization of signals it discuss about how the dataset are obtained and treated. In the statistical analysis correlation analysis is used to know the consistency of adsorption of metals on the sediment particles. Chapter 6.2.1 “Statistical analysis” describes in brief about the correlation analysis and how they are calculated on this dataset of sediment particles.

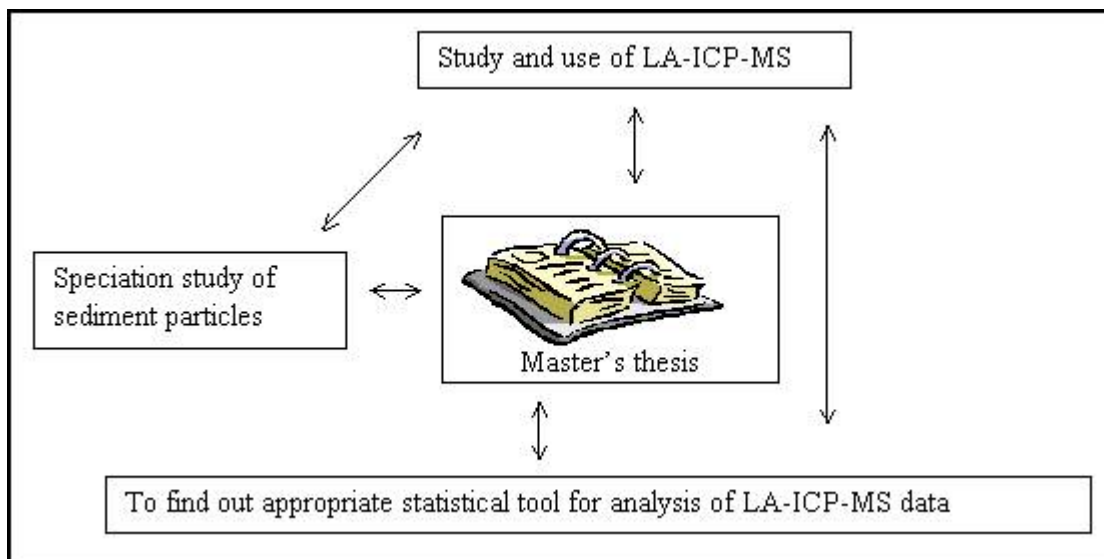


Figure 1: Schematic diagram of the objectives of this study.

2 Importance of speciation in analytical chemistry

Growing human activities have resulted in increased environmental pollution and complexity of the pollutants. It has been realized that the study of the environmental pollution as well as the chemical mechanism undergone and ongoing on component of the earth need to be studied in-depth. Moreover, the determination of different species of trace elements in environmental and biological materials is crucial in determining the toxicity of an element and its behaviour as they are dependent of chemical form and concentration [Kot and Namiesnik, 2000; Gleyzes et al, 2002]. Previously, most of the toxic and essential elements like mercury, lead, cadmium, arsenic and magnesium etc. were analysed as total content on the sample [Kot and Namiesnik, 2000]. Scientists have realized that this information is insufficient to characterize the elements in terms of toxicity and biochemical mechanisms which are dependent on the chemical form of an element or more precisely, the redox properties of the element on the environment of concern and the quantity [Tessier et al., 1979; Mester et al., 1998; Kot and Namiesnik, 2000; Yu et al., 2001]. For example, it is considered that the free ionic forms of metals like Cu, Cd, and Al are highly responsible for the toxic effect to aquatic biota and humans rather than complexation with natural ligands [Fytianos, 2001]. Moreover, toxicity and bioavailability could be more complicated based on the aquatic environment and the available chemical species itself and others [Fytianos, 2001]. The word elemental speciation or elemental speciation analysis has been thus coined to represent the study of the properties of element as mentioned above. Notwithstanding, it is also noted that the last 20 years of speciation analysis has seen the abuse of the term speciation or speciation analysis [Lobinski, 1998]. To cease the misuse and renderness, IUPAC has validated the term speciation or fractionation as “the process yielding evidence of the atomic and molecular form of an analyte” [Lobinski, 1998; Kot and Namiesnik, 2000; Gleyzes et al., 2002]. Furthermore, speciation is defined as the “term to describe the state of distribution of an element among different chemical species in a real world system (sample) and identify these species” [Lobinski, 1998]. Moreover, Lobinski, 1998 has addressed three points that the speciation work should incorporate. The first point is the environmental sample, which should not be spiked matrix. The second point is focused on defining the target species from the chemical viewpoint, and addressed that the operationally defined fractionation should not called speciation analysis. Finally, the last point is focused on defining a class of species in frame of which the analysis is to be carried out [Lobinski, 1998.]. In the present context, speciation analysis plays a vital role in the field mentioned below [Lobinski, 1998; Kot and Namiesnik, 2000]:

1. Study of biogeochemical cycles of chemical compounds in the three component of earth- aquatic, soils/sediments and atmospheric;
2. Determination of toxicity to the living being specially humans and chemical forms of elements present on the above component;
3. Analysis of food products;
4. Research in medicine and pharmaceutical products;
5. Impact of natural and human activities in the environment.

In the aquatic environment speciation of the metals depends on different forms including: free metal ions, labile metals coupled with organic complexes, metals permanently coupled with organic complexes, labile metals coupled with inorganic complexes, metals permanently coupled with inorganic complexes, metals absorbed in organic matter, and metals absorbed in inorganic matter.

Based on the toxicity and the environmental relevance, most commonly studied bulk and trace elements are As, Cd, Pb, PGEs, Fe, Cu, Mn, Mg, Al, Zn, Cr, Se, Sb etc. Brief descriptions of some of the elements are as follows:

Aluminium: The toxicity of the aluminium has been widely accepted although all chemical forms of aluminium are not homogeneously toxic [Das et al., 2001]. This is the reason why most of the scientists have accepted the necessity of speciation study of aluminium [Bloom and Erich, 1996]. Although the toxicity of the complexed form is reported to be less toxic than the inorganic one [Das et al., 2001], different toxic effects have been reported depending on different species. Fluoride-complexed aluminium is found to be more toxic than the organically complex aluminium and on the other hand less toxic than the aquo and hydroxy forms to the aquatic biota [Bloom and Erich, 1996]. The main reactive Al species of environmental concern are Al^{3+} , $\text{Al}(\text{OH})^{2+}$, $\text{Al}(\text{OH})_2^+$ and $\text{Al}(\text{OH})_4^-$, whereas $\text{Al}(\text{SO})^+$ and Al-humate are also reported to be present significantly in the aquatic environment [Das et al., 2001]. Because of the complexity of the aluminium in the aquatic environment, soluble aluminium has been classified as reactive [Das et al., 2001], inorganic, organic- fine colloidal mineral aluminium and aluminium associated with organic macromolecules, fulvic and humic acids, labile, non-labile, moderately labile, and monomeric etc [Bloom and Erich, 1996].

Cadmium: Cadmium is toxic at elevated concentration in the environment [Xue and Sigg, 1998]. Studies have focused on the complexation of cadmium with natural organic ligands in the aquatic environment although the knowledge of cadmium speciation is largely lacking [Xue and Sigg, 1998]. Speciation of cadmium in fresh water is dominated by the oxidation status and the pH of the element containing medium (surrounding environment), concentrations of numerous organic and inorganic anions and other metal cations. The mobility of cadmium in sediments is controlled by the adsorption of clay minerals, organic matter, and the hydroxides of iron and manganese [Bewers et al., 1987]. Furthermore, free Cd^+ , which control Cd-organism interactions, is more toxic than the total concentration with respect to availability [Xue and Sigg, 1998]. Chemical species like free ion, inorganic and organic complexes present in the solution are the result of its availability and mobility in the sediments [Xue and Sigg, 1998]. However, most of the speciation studies of cadmium have been studied combining the elements with other elements like Cu, Co, Fe, Mn, Ni, Pb and Zn [Das et al., 2001].

Copper: Copper is toxic when excessive intake occurs although trace amount of copper is an essential element [Das et al., 2001]. Free ionic form of copper is most toxic to aquatic biota and the toxicity of this metal ion decreases as the complexation by natural ligands occurs [Fytianos, 2001]. Most of the speciation studies of Cu have been focused on free copper ion rather than total concentration [Das et al., 2001]. Furthermore, most of the

speciation studies of copper are combined to the study of other elements like Cd, Co, Fe, Mn, Ni, Pb and Zn [Das et al., 2001]. It has been realized that the photochemical reactions are important for the speciation of the redox metals particularly copper, chromium and iron. Cu (I)/Cu (II) is found to be affected by the photoreduction process in the presence of Fe (I)/Fe (III), dissolved and colloidal organic compounds [Glazewski and Morrison, 1996]

Iron: Two inorganic form of iron i.e. Fe (II) and Fe (III) have been dealt abundantly in the speciation analysis [Das et al., 2001] and are important because of redox reactions occurring on environmental and biological systems [Zoorob et al., 1998]. Iron and manganese oxides are important for the speciation study of sediments as they have high adsorption capacities compared to other oxides such as Al and Si oxides [Guo et al., 1997; Bilali et al., 2002]. Similarly, their oxides are highly affective for the mobility of metals in lake sediments as they precipitate under oxic conditions and dissolve under anoxic conditions [Bilali et al., 2002]. For the elemental speciation studies, not only the study of free Fe (II) and Fe (III) ions are significantly important, rather the study of other forms like hydroxyl and other compounds of this metal are also important as their presence help and contribute to stabilize Fe (III) [Das et al., 2001].

Lead: Organometallic form of lead is considered more toxic than the inorganic form [Kot and Namiesnik, 2000; Das et al., 2001;] and is easily absorbed by the animals [Das et al., 2001]. Within the organic-lead complexation, presence of alkyl-leads are of great concern as they are highly toxic among which tetraethyllead, tetramethyllead and the complexation compound i.e. methylethyllead are most important [Zoorob et al., 1998]. The presence of oxic environment on the sediments enhances the accumulation of lead on the sediment particles, as they are highly reactive to oxide particles [Alexander et al., 1998]. Moreover, remobilisation of lead occurs in the water column and the sediment-water interface during the dissolution of redox sensitive particles like hydrous iron oxides [Alexander et al.; 1998]. Similarly, lead could be removed from the anoxic zone precipitating with lead sulphide (PbS) or by adsorption on FeS.

From the above brief descriptions it can be seen that all trace elements have the possibility of reacting with each other forming the complex compounds and could affect the complexation process with other elements as well. All these facts indicate the necessity of detailed speciation analysis of the metals in the aquatic systems.

3 Limitations of Sequential Extraction

Before entering the analytical procedure i.e. LA-ICP-MS technique, which is applied in this speciation study it could be better to have a brief idea about the limitations of vastly used analytical procedure i.e. sequential extraction procedure, which is used before the application of LA- ICP-MS technique. About two decades ago, a sequential extraction procedure is considered as one of the major analytical techniques in the field of elemental speciation analysis. Later on it is realized that this analytical techniques have some difficulties on the study of trace and ultratrace elements. From the very beginning of the use of the sequential extraction procedure many investigators have marked the pitfalls of it mainly due to the lack of selectivity/uniformity of reagents, readsorptions, and redistributions of metals solubilised during the extraction, sample pre-treatment, and general methodology to make the analytical procedure and result acceptable [Kot and Namiesnik, 2000; Gleyzes et al., 2002].

3.1 Lack of selectivity of reagents

Various kinds of reagents are used as an extractant to dissolve selective mineralogical phases of the metals from sample. Many theoretical and experimental works applied on synthetic and natural solid materials had shown the lack of selectivity of reagents [Gleyzes et al., 2002]. Yousfi and Bermond (1997) demonstrated the lack of selectivity exemplifying the case of Pb [Yousfi and Bermond, 1997]. Recovery of lead was studied from a spiked organic fraction and an iron oxide reaction under BCR extraction procedure. In the experiment, 40% of the total lead for humic acid was found in the second step (hydroxylamine) whereas 50% was in the first step (acetic acid/ acetate) for iron oxide. Furthermore, sequential extraction was criticized stating that the reagent selectivity was suitable for the evaluation of metal co-precipitated phases but not for the metal sorbed phases [Ariza et al., 2000]. As a concluding remark, Berman stated that pH and changes on it were probably one of the major parameters, which was responsible for the unresolved problems of sequential extraction procedures [Bermond, 2001].

3.2 Readsorption and redistribution

Readsorption and redistribution of some metals were the result of incomplete dissolution of some phases and the change in pH [Kheboin et al., 1987; Gleyzes et al., 2002]. These problems were experimented by applying Tessier's scheme to mixed synthetic models where each step was spiked with specific trace elements [Kheboian and Bauer, 1987]. Extraction results for sediment containing Pb, Cu, Fe, Zn, and Si were analysed. On application of the model, Pb should be extracted on fraction 2 (bound to carbonates), Cu on fraction 3 (bound to Fe/Mn oxides), and Zn on fraction 4 (bound to organic matter). On contrary, significant amount of Pb was extracted on late fraction and Zn on fraction 2 and 3. In the case of Cu it was found untouched in fraction 3. Other authors also reported the redistribution of Pb [Gleyzes et al., 2002]. Furthermore, it was reported that the

redistribution and readsorption of Pb, Cu and Zn were significant only for elevated initial contents of these elements [Gleyzes et al., 2002]. Moreover, lack of selectivity was also considered as a responsible factor for metal redistribution [Gleyzes et al., 2002]. Comparing the two extraction procedures- Tessier et al.'s and the three stage BCR procedures, it was found that the first procedures yielded the highest portion of lead at reducing step whereas the later one yielded at the oxidizing step [Raksasataya et al., 1996].

3.3 Sample pre-treatment

It was reported that the errors could be the result of chemical modifications occurred during the drying step of sample preparation and the treatment time [Gleyzes et al., 2002]. As cited by Bordas and Bourg (1998), the natural relation of sediments with the surrounding environment could be disrupted due to change in the redox potential, temperature, pH and pressure modifying the physico-chemical composition of the sediment [Bordas and Bourg, 1998]. Widely used methods for the sample preservations like air drying (60, 70 or 150 degree) and freeze-drying were found not to be able to preserve the sample's integrity especially the distribution of Cu, Pb, Zn, and Cd on their low content [Bordas and Bourg, 1998; Davidson et al., 1999].

3.4 Methodology

Operating conditions like the extraction time, the solid-to-liquid ratios, the type of agitation, the methods used for solid-liquid separation, the mass of the test sample and the rinsing methods were also found to be determinant for influencing the reaction efficiencies [Gleyzes et al., 2002]. As an example, in the case of iron oxides, it was reported that the dissolution was incomplete during the Tessier's scheme leading to over estimation of the residual fraction [Gleyzes et al., 2002].

Whatsoever, the sequential extraction procedure was criticized mentioning its limitations; the criticism was questioned by various authors [Gleyzes et al., 2002]. Tessier et al, 1979 has mentioned that despite the rapidity and simplicity of sequential extraction, these techniques suffer from the difficulty of finding a single reagent effective in dissolving quantitatively the non-residual forms of metal without attacking the detrital forms.

LA-ICP-MS has been used to determine the elemental association in samples as small as 50µm in diameter and to provide elemental fingerprinting [Walting et al. 1997]. It has solved a problem of elemental dissolution faced in the sequential extraction technique. Dissolution technique prior to analysis can be time consuming and depending upon the thermolability of the analyte, elemental loss through different volatilisation capacities as well as inertness of certain elements is possible which is prevented by the use of LA-ICP-MS [Walting et al., 1997]. Nonetheless, use of LA-ICP-MS provides the detail fingerprinting profile of different elements in sample particle keeping its heterogeneity intact, which is not possible in sequential extraction technique.

4 Instrumentation of LA-ICP-MS

Need for a well established, powerful, rapid and very sensitive method for trace and ultra-trace multi-elemental analysis is fulfilled by laser ablation inductively coupled plasma mass spectrometry [Klemm and Bombach, 2001]. The process of progressive and superficial destruction of a material by melting, fusion, sublimation, erosion, and explosion etc. by means of laser is called laser ablation [Gunther et al., 2000]. Houk et al. first demonstrated a combination of Inductively Coupled Plasma (ICP) with a quadrupole Mass Spectrometer (MS) for elemental analysis of aqueous sample solutions, which is later on known as ICP-MS [Durrant, 1999]. First commercial ICP-MS instrument was launched in 1983-84 and has gained wide acceptance making it as a standard tool/method for multi-elemental and isotope ratio analysis of diverse biological and geological samples [Durrant, 1999]. In 1985, Alan Gray introduced the first combination of laser ablation to ICP-MS, known as LA-ICP-MS [Gunther et al., 2000]. Two major fields of application has been identified for the use of LA-ICP-MS i.e. bulk analysis with a low spatial resolution of 80-350 μm crater diameter and local analysis with a high spatial resolution of 4-80 μm crater diameter [Gunther et al. 2000] The LA-ICP-MS instrument used for this analytical study was Ceta LSX-200 Laser System Coupled to Elan 6000 ICP-MS.

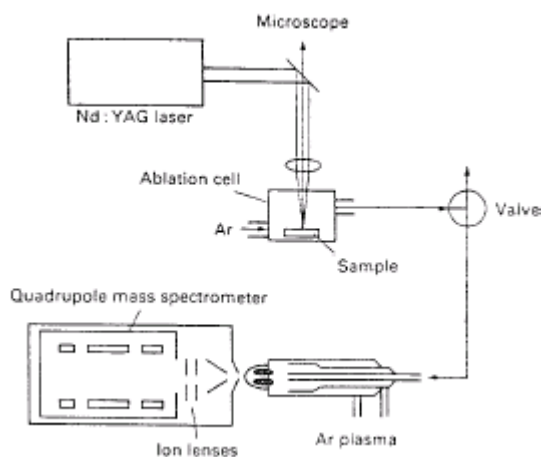


Figure 2: Schematic diagram of the LA-ICP-MS system. Adapted from Durrant, 1999.

4.1 Principle of laser ablation system

The laser ablation system consists of a laser source, some ancillary optical devices like lenses, camera and a sample cell. Figure 2 represents the schematic diagram of the laser ablation system combined with ICP-MS. Different components of the LA-ICP-MS are briefly described below:

4.1.1 Laser source

Monochromaticity, spatial and temporal coherence, lasers beam with low divergence and high directionality, as well as high radiance are the characteristics feature of laser [Gunther et al., 2000]. Lasers are composed of three parts i.e. energy input, amplification in an active medium, and light output. Among the two classification of laser types-continuous wave (CW) and pulse wave; pulse wave is widely accepted for ablation rather than the continuous one [Gunther et al., 2000]. The benefit of pulse wave is that it allows input of high-energy short pulses so the concentration of energy over a short period of time is possible [Gunther et al., 2000]. The first laser source used for the ablation was ruby laser [Durrant, 1999; Gunther et al., 2000]. The success of the ruby laser has led to the development and use of Nd: a YAG laser system which is of solid active medium laser type [Gunther et al., 2000] produced by a rod shaped- crystal of Nd^{3+} doped Yttrium Aluminium Garnet ($\text{YAl}_5\text{O}_{12}$). Most of the recent analytical research work utilizing the LA-ICP-MS consists of Nd: YAG systems as they are relatively simple and cheap [Durrant, 1999; Gunther et al., 2000].

Nd: YAG lasers operating at 1064 nm, 532 nm, 266 nm and 213 nm have the energy range of 0.2-550mJ, 0.9-70mJ, 0.01- 40mJ and 7.5 mJ respectively. The energy required and the wavelength of laser are interlinked with each other and are different from the ruby laser system and the Nd: YAG laser system. Figure 3 represents the energy level for the Nd: YAG laser effective for the ablation of the sample [Durrant, 1999].

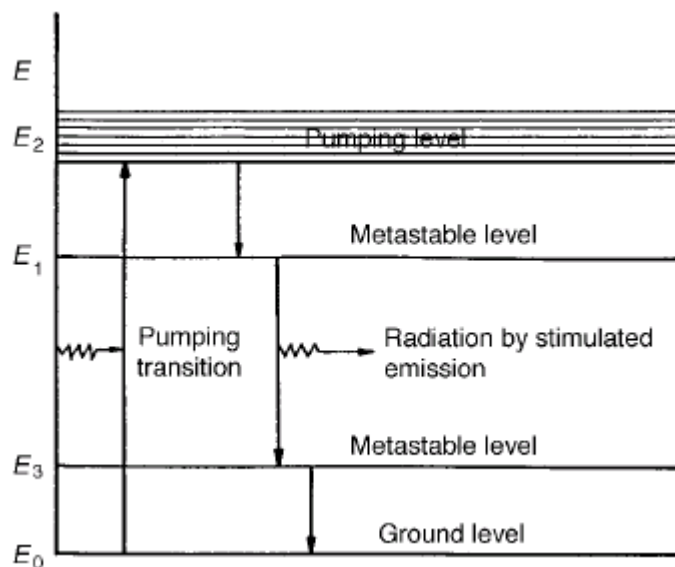


Figure 3: Energy level diagram for Nd: YAG laser. Adapted from Durrant, 1999.

The most commonly used wavelength for pulsed ablation is of energy ranging from 10mJ- 300mJ at 1064 nm [Durrant, 1999]. The Nd: YAG laser system can be operated in two pulse modes, the free running mode (μs pulse duration), which is also known as N-

mode and Q-switched mode or Q-mode (ns pulse duration). The ablation process can be performed in the infrared (IR) and ultraviolet (UV) wavelength lasers. Notwithstanding, Nd: YAG can provide the UV wavelength on addition of an optical device as its primary wavelength falls under the category of infrared wavelength [Gunther et al., 2000].

4.1.2 Optical devices

Optical devices are important for determining the laser spot size as well as for processing the beams like focusing, spatial filtering and homogenizing [Gunther and Mermet, 2000]. Figure 4 represents the schematic diagram of the optical instruments arranged in the Nd: YAG laser ablation system at 266nm where the energy level is up to 100mJ

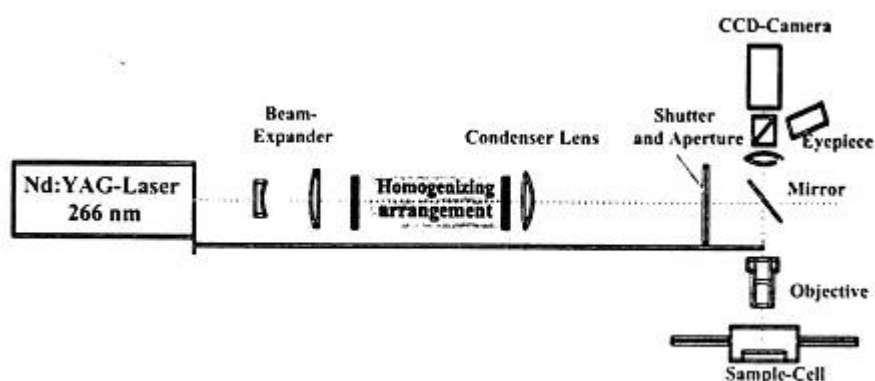


Figure 4: Schematic diagram of the arrangements of optical devices. Adapted from D. Gunther et al.

The focusing objects are of mainly two categories- refracting and reflecting types. However, large range of models are also available based on analytical requirements like laser wavelength and power, magnification, focal spot size required, working distance, achromaticity, and cost [Gunther et al., 2000]. As it is a known fact that IR and UV wavelength are harmful for human eyes, the use of monitor and simple or high magnification optics like TV- camera and microscope allows the indirect but efficient monitoring and analysis of the ablation process as well as the efficient and in-depth analysis of the smaller grain size also.

4.1.3 Sample cell and transportation system

Designing of sampling cell can be different for different analytical applications. However, the cells must have three efficient categories: swift reach of laser to sample, a port for carrier gas to enter the sampling cell and a port to sweep out the ablated material by carrier gas to ICP-MS. Moreover, a closed gas tight cell is very important to block the mixing of atmospheric gases, which can give rise to anomalies due to contamination. Figure 5 represents the schematic diagram of the sampling cells and transportation port.

In a LA-ICP-MS having sequential quadrupole mass analysers, cell volume and transfer tubing must be coherent and sufficient to allow dilution, mixing and transportation of sample pulses. This helps the ICP-MS to receive fairly stable input of sample [Gunther et al., 1999]. Moreover, the sample cell must be able to accommodate many samples for analysis along with calibration and reference materials. This reduces the frequency of opening the cell as well as maintains constant ICP operating conditions [Gunther et al., 1999]. Furthermore, vertical laser to the sample can give rise to the harmful back reflections to the incoming laser. So the sample holding ablation cell window is often slanted at 45° to the vertical of the incoming laser to reduce the back reflection [Durrant, 1999; Gunther et al., 1999].

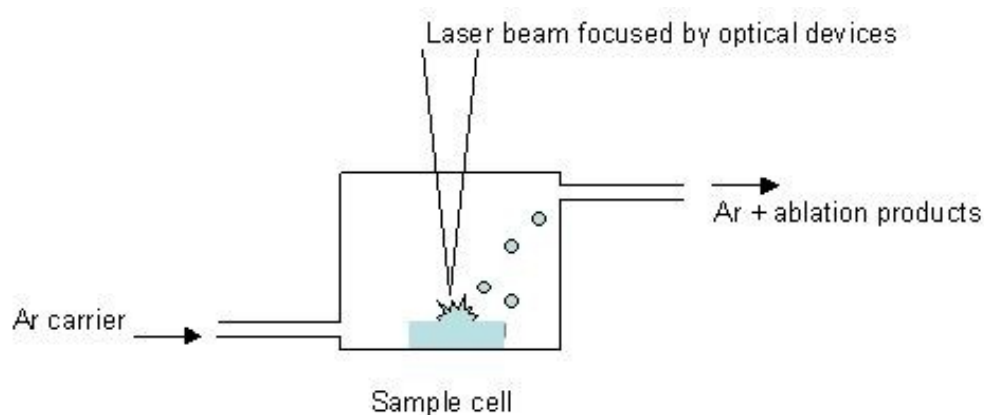


Figure 5: Schematic diagram of the sampling cell and transportation port.

Sampling cell is a place where interaction between the incoming radiation and the solid sample occurs. This interaction is dependent of different variables related to the laser, physical properties of solid sample and the atmosphere i.e. wavelength, energy, spatial and temporal form of the laser beam and the heat capacity, heat of vaporization and the thermal conductivity of the sample [Arrowsmith, 1987; Durrant, 1999]. When the incoming laser energy strikes the sample the converted heat energy leads to melting, then boiling and vaporization of impacted sample. The time required for the vaporization of the sample is given by

$$t_v = nKpC(T_v - T_o)^2 / 4P^2 \quad (1)$$

Where, t_v = Time of vaporization
 K = Thermal conductivity;
 P = Mass density of sample;
 C = Heat capacity;
 T_o = Initial temperature;
 T_v = Vaporization temperature of sample;
 P = laser power density.

From above equation it can be seen that the different material has different vaporization time as K, C and T is dependent of material composition.

After the ablation, generally ablated particle on the sample cell mixing with argon acquires the spherical shape. The spherical particles thus formed are then transferred to ICP-MS. Particles of diameter less than 5 nm have been found to result in low transport efficiency as they tend to be lost by diffusion. Similarly, the efficiency is lower for the particles larger than $3\mu\text{m}$ as they could settle out under the gravitational effect. Particles within a range of 5nm and $3\mu\text{m}$ are carried with an efficiency of greater than 80% [Durrant, 1999]. Moreover, using the large diametric transport pipe could minimize collision of particles with wall thus reducing the chances of being lost. Large diameter allows the increased ratio of gas column to wall area reducing the memory effect [Gunther et al., 1999]. On the other hand, a small diameter is preferred to increase the linear gas velocity (cm/s), which reduces the time of flight and gravitational settling [Gunther et al., 1999]. All these factors mentioned above are important while optimising the instrument.

4.2 ICP-MS for laser ablation

Before introduction of the Inductively Coupled Plasma Mass Spectrometry (ICP-MS) three main analytical techniques were used. ICP-AES (Inductively Coupled Plasma Atomic Emission Spectrometry) as a multi-elemental technique has detection limits at parts per billion (ppb) levels for most elements. Similarly, FAAS (Flame Atomic Adsorption Spectroscopy) as a mono-elemental technique has a detection limit at ppb or higher and GFAAS (Graphite- FAAS) as a mono-elemental technique has detection limits at sub-ppb level for many elements [Beauchemin, 2000]. In 1978, the first mass spectra from an ICP were obtained whereas the first commercial instrument was introduced in 1983 [Rauch, 2001]. ICP-MS is a method of choice for the analysis of trace metals in a number of matrices including environmental and biological samples [Rauch, 2001].

4.2.1 Instrumentation of ICP-MS

Most of the commercial ICP-MS uses Argon gas (Ar) as a plasma ion source, whereas He is also used as a plasma source based on the analytical requirements. At high temperature the incoming gas is converted to a highly ionised form called as plasma. Argon flows through a radio frequency magnetic fields induced by a coil wound around the end of the quartz torch generating plasma of 1-2.5Kw [Beauchemin, 2000]. Basically, ICP-MS consists of three concentric quartz tubes: an outer tube or main tube for the plasma, an intermediate or auxiliary tube for the auxiliary gas, and central tube or injector tube for the carrier gas which is also called as nebuliser gas when a nebuliser is used for the introduction of solutions. The argon from main flow is fed with electrons produced by high voltage spark, which on collision with it causes ionisation and plasma ignition. Moreover, the outer gas acting as a plasma source is used to maintain the plasma along

with a radio-frequency (rf) power supply stabilizing it and to prevent the plasma from melting the outer tube. The auxiliary gas flow maintains the control over position of the plasma and pushes it away from the torch as well as prevents plasma from overheating the rim of the inner tube. The third flow or carrier gas carries the sample and introduces it into the center of the plasma. As the transfer of energy occurs without the use of electrode, this energy transfer is called inductively coupling. Similarly, collision of Ar atoms with the electrons and ions in motion, which is continuously induced by the oscillating magnetic field, results in the ohmic heating of gas resulting in temperatures 6000-10,000K [Beauchemin, 2000; Rauch, 2001].

After the introduction of sample in plasma, it goes through several processes in milliseconds [Beauchemin, 2000]. The foremost process is the desolvation process of each droplets where the solvents are evaporated and results in an anhydrous salt. Then it follows by vaporization, which involves the physical transformation of the salt particles from solid to gas phase. The preceding phase is atomisation of the gaseous molecules into free atoms and finally the conversion of atomised molecules to ionic form i.e. ionisation process. Ionisation process is proposed to occur by three possible mechanisms: electron impact ionisation, charge transfer and penning ionisation [Beauchemin, 2000]. The electron ionisation occurs when the analyte, M, collides with the free moving electrons (eq.2). For this ionisation the kinetic energy of the colliding electron must be greater than the threshold energy for ionisation.



Ionisation through charge transfer can occur when the total energy needed for ionisation and excitation of analyte, M, is less than the first ionisation potential of argon (15.76ev) (eq. 3). The ions thus formed then remains in an excited electron.



Whenever the collision of analyte, M, with metastable argon atom, Ar^m , occurs, it gives rise to the penning ionisation (eq. 4). However, this mechanism is not favoured as the first two-ionisation process due to low population of metastable argon compared to that of electrons and Ar^{+} in the ICP.



The ions thus formed in the high-pressure atmospheric plasma are then transferred to the mass spectrometry detector operating under vacuum at room temperature. In viewing this critical condition, interface is used to allow only ions to the detector. The interface consists of an outer sampler cone and an inner skimmer cone with millimetre orifices through which the ions are extracted from plasma. Since there is a captive coupling between the rf coil and the plasma, it produces a potential difference of a few hundred volts. This can create electrical discharge, which is called as a secondary discharge or pinch effect between the plasma and sampler cone [Beauchemin, 2000]. Furthermore, this discharge increases the reformation of interfering species as well as affects the kinetic

energy of the ions entering the mass spectrometer. Thus using the rf coil whose design can vary on different instruments reduces this electrical discharge. After the extraction of ions from the interface region they are directed to the main vacuum chamber by series of electrostatic lenses called ion lenses. These lenses function to focus the ion beam electrostatically and to stop photons, particulates, and neutral species from reaching the detector. Otherwise, the photons can increase signal noise. The ions are then introduced to the mass filter, which acts depending on mass-to charge ratio (m/z) of ions. Most commonly used quadrupole mass analyser acting as mass filter consists of four metal or metallised rods suspended parallel to central axis with opposite pairs connected together. On application of direct current and rf voltages, only ions with a specific m/z ratio will acquire a stable trajectory and emerge to the other end of the quadrupole for detection (Figure 6)

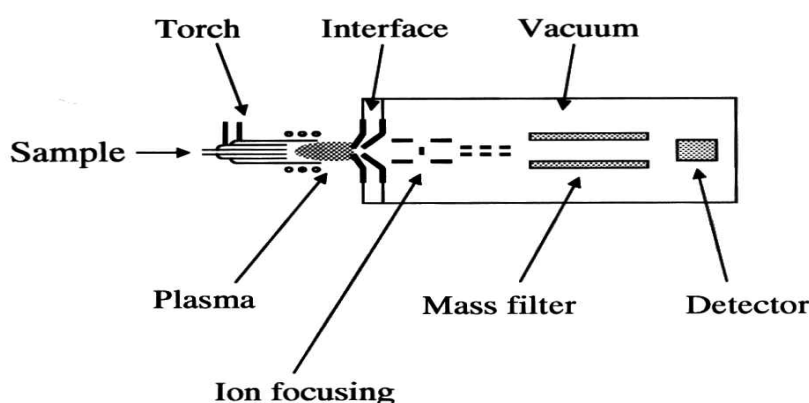


Figure 6: Schematic diagram of quadrupole ICP-MS. Adapted from Rauch, 2001.

Since the ICP-MS is capable of detecting wet aerosols, the solid samples are vaporized by the use of laser ablation and detected by ICP-MS.

4.3 Limitations of LA-ICP-MS

Laser parameters, transportation system and carrier gas is found to be influential on the elemental partition [Beauchemin, 2000]. Laser wavelength, output energy/pulse energy, frequency and pulse width have combined or individual effect on sample like dissipating heat into the sample, quantity of ablated material, crater depth and particle formation. Similarly, cell volume, tube length and diameter on transportation system have effect on plume expansion, particle agglomeration, particle separation and particle loss. The viscosity and flow of carrier gas affects the energy transfer onto the sample surface, plume formation, particle density and transportation efficiency.

In the field of precision and interference, ICP-MS has shown some limitations. However, for the low-resolution instruments spectroscopic interferences are major whereas non-spectroscopic interferences are common on all instruments [Beauchemin, 2000].

Short-term precision is limited by noise in the ICP-MS, which is a result of interaction of plasma and interface. The noise responsible for degrading the precision depends on the design of the instrument.

Spectroscopic interference, which results from isobaric overlap of isotopes of different elements, polyatomic ions and double charged ions are a major problem in quadrupole based ICP-MS. When two elements have isotopes of essentially the same mass then isobaric overlap occurs [Rauch, 2001]. Most isobaric interferences between the elements like that of $^{114}\text{Sn}^+$ on $^{114}\text{Cd}^+$, except those originating from the plasma like that of $^{40}\text{Ar}^+$ on $^{40}\text{Ca}^+$ can be corrected by the software [Beauchemin, 2000]. The software measures the signal of an interference-free isotope of the interfering element for e.g. Sn. Then it applies a correction factor, which is based on the natural abundances of isotopes and subtracts that contribution from the analyte signal, thus yielding the interference-corrected analyte signal.

When most common element in the plasma and the sample matrix like Ar, H, O, N, combines with other elements they can form ions having the same nominal mass as an analyte ions, which are called as polyatomic ions. Moreover, this interference may arise from the matrix including any reagent used during sample preparation, for e.g. chlorine containing acids resulting in the formation of $^{35}\text{Cl}^{16}\text{O}^+$ and $^{40}\text{Ar}^{35}\text{Cl}^+$ responsible for interfering with V, ^{15}V and monoisotopic ^{75}As respectively.

Possible formation of double charged ions, which results when the second ionisation energy of an element is lower than the first ionisation energy of Ar, also give rise to the interference [Rauch, 2001]. Interference due to double charged ions occurs when an element is to be determined at mass to charge ratio as of double charge ions have half the ratio of mass to charge than the single charged ions. However, the effects of doubly charged ions are generally less severe [Beauchemin, 2000].

Some approaches reported to reduce the spectral interferences are the use of sector field instrument with a sufficient mass spectral resolution, reaction or collision cells, matrix separation prior to analysis, alternative sample introduction systems and mathematical correction [Rauch, 2001].

Non-spectral interference is more susceptible [Beauchemin, 2000], complex and less understood [Rauch, 2001]. These interferences have been reported as suppression of analyte signals or enhancement effects and physical effects caused by dissolved solids [Rauch, 2001]. However, use of an internal standard that closely matches the properties of the analyte helps to overcome this interference.

5 Experimental methodology

5.1 Sampling and sample preparation

5.1.1 Sampling

Sediment samples were collected from Mölndal River in Göteborg, Sweden in September 1998. The river runs through industrial and urban areas stretching alongside the busy traffic way. Sampling was done as a part of a project started in 1997 to carry out the study of effect of industrial and urban areas as well as traffic on the urban river sediments [Rauch, 2001]. Surface sediments of about 20-30mm were sliced so as to get the oxic sediments. The samples were then kept in a cleaned polyethylene container to avoid further contamination and later carried to the lab. As soon as the sediments were carried to the lab, it was wet sieved with ultrapure water (Barnstead Nanopure) to sort out the different grain size for the analysis. Grain size fractions of 63-125 μm were chosen optimum size for further investigation and thus dried at 105°C. The sediments were stored in the polyethylene containers for further future analysis. Adsorption of trace elements on the sediment particles increases as the grain size decrease and vice versa [Stone and Droppo, 1996]. Smaller grain size provides a high adsorption sites to the elements in compare to big particles. The reduction of the particle size less than the 63 μm reduced the precision of the micrometric analysis as well as required more effort and glue solution to prepare the sample [Klemm and Bombach, 2001].

Notwithstanding, it was noticed that the concentration of the Pb in the Mölndal River was related with the urban automobile sources used before the phase down of leaded fuel. Decreased Pb concentration was reported in the Mölndal River after the phase down of leaded fuel [Rauch et al., 2000].

5.1.2 Sample preparation

Various methods are available for the sample preparation for the analysis of the LA-ICP-MS. However, the LA-ICP-MS is considered as a less time consuming technique in terms of sample preparation, uses of glue solution like methacrylate resin needs time to fix the particle grains to be analysed [Klemm and Bombach, 2001]. River sediments were fixed on the regular sticky tape to ease the ablation procedure (Figure 7). Particle grains could be seen with ease so as to carry out line ablation for the elemental associations and preferred to pellets as it allows the high resolution of individual particles [Rauch et al., 2000].

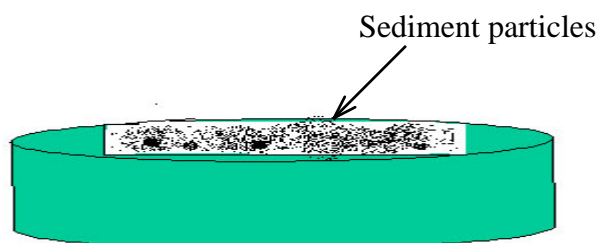


Figure 7: Schematic diagram of sample preparation used for the ablation of sediment particles.

5.2 Instrument and operating conditions for analysis

Cetac LSX-200 systems (Cetac, Omaha, NE, USA) coupled with Perkin Elmer Sciex Elan 6000, which is situated at Chalmers University of Technology was used for this study (Figure 8). The laser used by LSX-200 was Nd: YAG laser with a frequency output of 1064. This frequency was quadrupled by a set of mirrors with a final output of frequency 266nm. Similarly, zoom ranging from 80xs to 800xs was attached with a video system allowing choices over ablation sites and particles. Moreover, Elan 6000 ICP-MS was equipped with a quadrupole mass filter and Fazel-Scott spray chamber as a cross flow nebuliser to form an aerosol. Teflon tube was used to carry out the sample from sample cell to the ICP-MS instrument. Ar was used as a carrier gas and plasma ion source. The instrument fitted with auto-sampler was run from outside the instrument chamber. LSX-200 laser system was also controllable by the computer system although situated outside the ICP-MS chamber (Figure 8). The parameters used for running the LA-ICP-MS for analysis of samples are listed below (Table 1):



Figure 8: Picture of ICP-MS (left) and LA-ICP-MS (right) used at Chalmers University of Technology, Sweden.

Parameter

- Laser

Operating Mode	Q-switched
Wavelength	UV 266nm
Ablation pattern	Line ablation
Energy level	1mJ
Spot size	10 μ m
Repetition rate	20Hz
Scan speed	1 μ m s ⁻¹

- ICP-MS

RF power	1000W
Plasma gas	Argon, 16.01 min ⁻¹
Auxiliary gas	Argon, 0.91min ⁻¹
Carrier gas	Argon, 1.01 min ⁻¹
Dwell time	5ms
Sweeps per Reading	25

Table 1: LA-ICP-MS operating parameters used for ablation of sediment particles

6 Results and Discussions

The sediment particles to be ablated were selected based on the size and colour. Sediment samples were found to be composed of dark grey to black particles as well as transparent quartz particles. Dark grey and black particles were preferred for ablation as they consist of more metals like Pb than on Quartz. The laser parameters were calibrated in viewing especially dark grey particles. Similar analytical work was also carried out and found that quartz was poorly ablated with the similar parameters as presented in Table 1. Beside that, elemental compositions were also considered while ablating the particles of interest. Results obtained from the LA-ICP-MS instrument and their analyses were further classified as normalization of signals and statistical analysis.

6.1 Normalization of signals

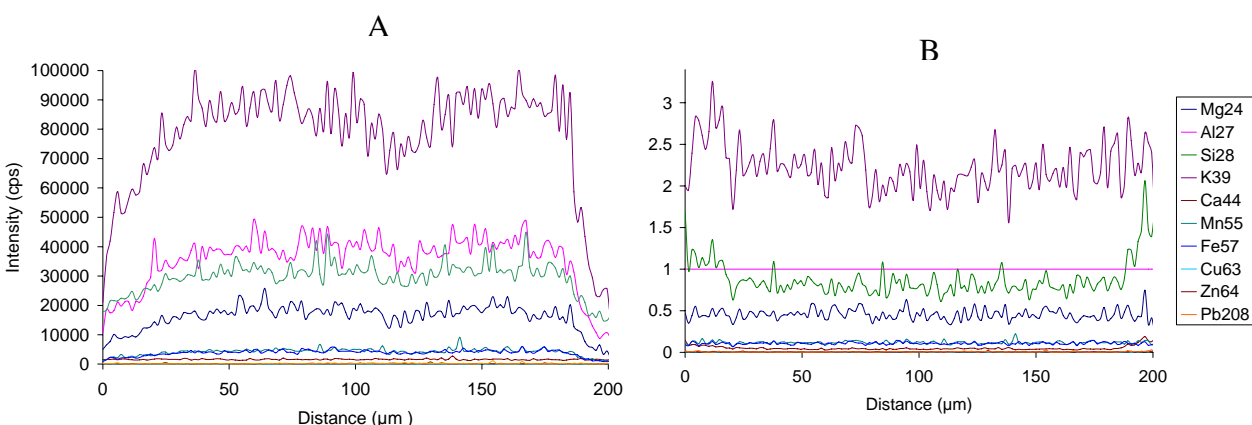


Figure 9: A- Elemental profile of sediment particles before normalization. B- Normalized elemental profile of sediment particle.

About 50 particles were ablated and it was found that some particles consist of intense peaks for certain elements like Al, K and Mg. Patchy signal peaks were obtained for all elements analysed thus suggesting a differential ablation behaviour (Figure 9-A). The influences of this differential ablation on elemental signals were corrected through signal/mathematical normalization [Rauch and Morrison, 2003]. For normalization, the signal of an aluminium element was used as its distribution throughout the particle was assumed to be homogenous. Notwithstanding, the particles with signal peaks of Al less than 2 million as well as less abundant were considered as less saturated and used for further analysis. Elemental profiles for the particles used in this analytical study are presented in Figure 18, Appendix I. Highly saturated peaks could affect the normalization procedure and distribution of other peaks of elements of interest. Al at the surface of earth is responsible for the association of particulate matter associated with soil/sediments [Driscoll and Postek, 1996]. Furthermore, aluminosilicates (Al_2SiO_3) are expected to have a core on the sediments and thus distribution is homogenous across the

surface and in depth [Rauch and Morrison, 2003; Tam and Yao, 1998]. However, iron was also found as a good normaliser for elements like Zn, Mn, and Ni, whereas Al for Cu and Cr [Tam and Yao, 1998]. Furthermore, as the scope of this work was not to compare specific elements as normaliser and considering all the factors mentioned above, Al was used for normalization (Figure 9-B). Al and Si as normaliser were also found to provide the same surface distribution supporting normalization of either element [Rauch and Morrison, 2003].

6.2 Statistical analysis

In speciation analysis, various approaches can be used to interpret the association of elements. Here, we used correlation analysis, percentage association of elements by counting the overlapping peaks and ternary plots. As one of the aims of this study is to identify a possible way of interpreting association or adsorption of elements, correlation analysis and ternary plots are focused. Correlation analysis is a widely used statistical tool to summarize the relationships between two variables. In this context, to be able to calculate the correlation and to see the relationships between them, each element in the particles is considered as variables. Correlation analysis also provides the idea about strength of linear relationship between different elements, which can be verified by drawing the scatter plots. To measure the relationships between the different variable elements, correlation analysis was carried out for the normalized results. In the present context measurement of correlation can be interpreted as the measure of the strength of binding possibilities of different elements on the particles. However, there are certain parameters to check before calculating the correlation coefficients, i.e. normal distribution and independence of the data.

Normal distribution:

Two kinds of correlation analysis can be carried out between two of variables: "Pearson correlation coefficients or "simple correlation coefficients" and "Spearman's rank correlation coefficients". It is to be noted that Pearson correlation is only applicable to the variables if they are distributed normally. It is also applicable between the variables if only one variable is distributed normally. If none of the variables are distributed normally then Spearman's rank correlation is applicable. Each variable elements measured in the particles were thus checked for the normality. It was found that most of the elements were not distributed normally. Pearson correlation is also applicable if the distribution is normal on its log phase. For those elements, which were not distributed normally, log value was taken and found that in most cases they were distributed normally. However, in some cases like the relation between S and Si, spearman correlation was calculated, as they were not normally distributed after taking log of their values also. One of the interesting facts observed during this calculation was that magnesium was distributed normally in two out of 12 particles.

Autocorrelation function (acf):

Correlation analysis is applicable to the independent variables and the observations are assumed to be independent. But this is not applicable in all the variables and sometimes time series data will be auto-correlated i.e. not independent within itself. The variables in time series were checked for autocorrelation. Various elements have shown various trends and in some cases it was found that they were significantly auto-correlated. Figure 10 represents a diagram of autocorrelation observed in one of the particles.

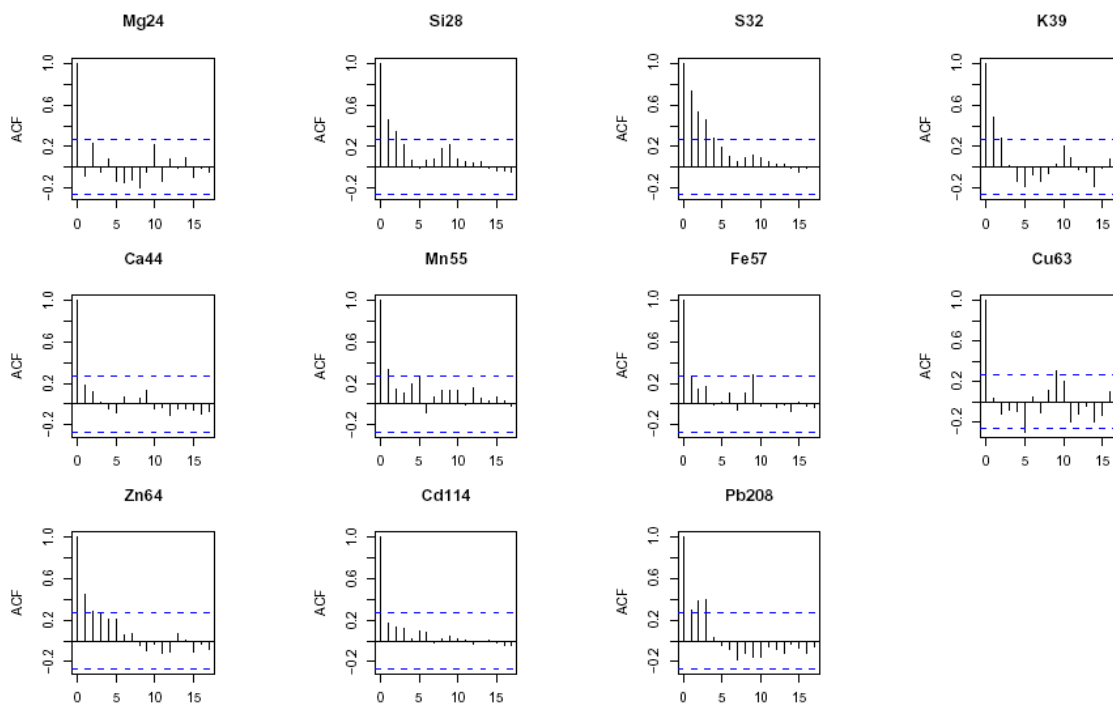


Figure 10: Elements showing different nature as observed for autocorrelation function vs. Lag-phase.

For a time series of length N , autocorrelation essentially reduces the number of independent observations to below N observation. In such a case the correlation equation should be altered to use an adjusted or effective sample size [Dawdy and Matalas, 1964]. In the context of elemental profiling on this work, elemental profile for each element on a particle represents one sample size and the time of each ablation was represented by sample point. Moreover, to calculate the effective sample size in time series, the autocorrelation in the series must be first-order autocorrelation (dependence in lag-1 only). As the x-axis represents the lag phase (order phase) it could be seen that some of elements were correlated behind lag-1 or first order observation also. Lag phase considered in this work while calculating the autocorrelation was represented by the time of ablation or sample point along the particle. In some of the particles S, Si, K and Ca are correlated significantly behind Lag-1 phase also. In such cases the relation between these elements with others were rejected. In the tables presented at Annex II, some of the elements not having correlation values indicated by “NA” were the result of significant

autocorrelation observed on those elements behind first order. One possible reason for this was due to softness of the particle element and the energy of the laser affecting the ablation of elements. This could possibly release high amount of elements in the sample chamber thus affecting further reading at other points. This finding can be important on optimising the LA-ICP-MS and verifying the significant coincidence of peak values.

Test for significances:

The t-test was applied to determine significant binding between various elements on the particles. On this significant test where α -level is 0.025 i.e. one tailed test, the hypothesis considered were as follows:

H0: Correlation coefficient is zero

H1: Correlation coefficient is greater than zero.

It should be noted that if the test is repeated several times and sample correlation is computed, the probability of getting at least one significant correlation is greater than the threshold r or alpha (α)-level [Dawdy and Matalas, 1964]. It was suggested that, in order to get the desired α -level, it should be divided by the factor k , which represents the number of correlation for each pair of elements or number of particles used for each pair of elements. On this analysis 12 particles were considered for correlation analysis after looking for normality and lag-1 phase. Thus the level of significance on this case was $a' = a / k = 0.025 / 12 = 0.00208$.

6.2.1 Correlation results

Different correlation coefficients and significances observed within and between the elements in particles at the level of $\alpha' = 0.00208$ were presented in Figure 11 and 12 as well as tabulated on Appendix II. Moreover, mean and deviations were also calculated to see the variance in the correlations coefficient of similar elemental pairs between particles. This study was specially focused on the association Pb with other elements. However, association of other metals were also studied, although not in detail as they compete with each other for binding sites.

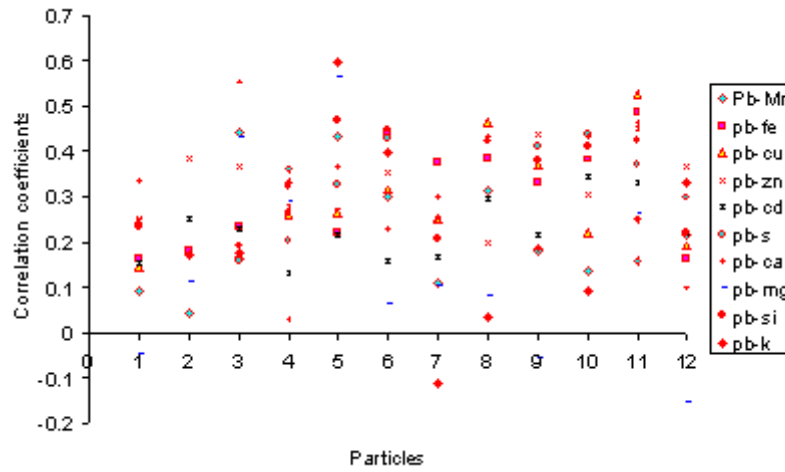


Figure 11: Correlation or association coefficients between Pb and other elements.

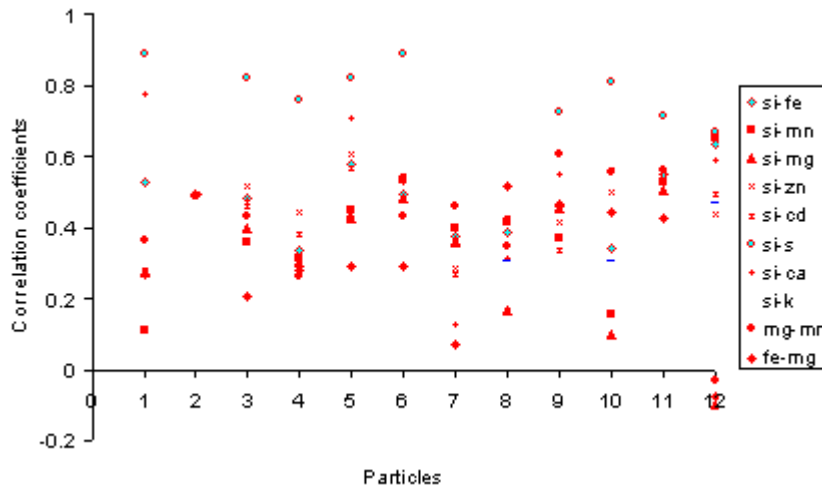


Figure 12: Correlation or association coefficients between different elements.

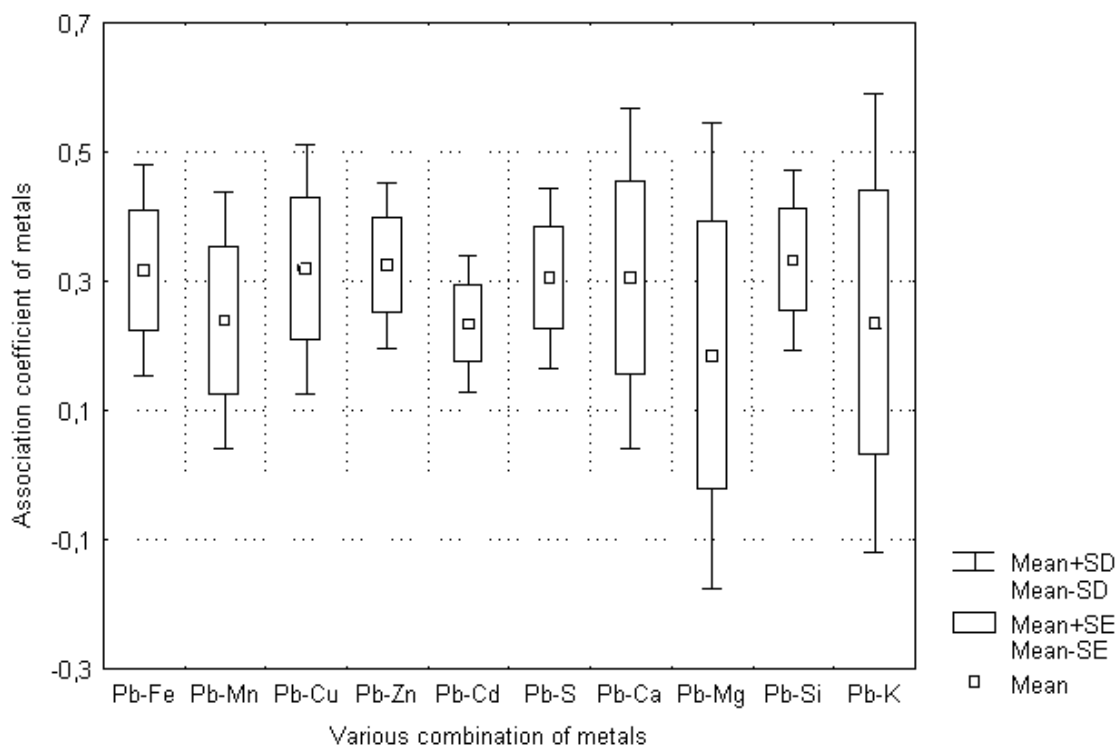


Figure 13: Mean correlation coefficient of Pb with other elements.

Significant mean correlation is observed between lead with other elements like Pb-Si ($r = 0.339$, std. Dev. = 0.107), Pb-Ca ($r = 0.329$, std. Dev. = 0.157), Pb-Zn ($r = 0.326$, std. Dev. = 0.07) followed by Pb-S ($r = 0.319$, std. Dev. = 0.102) and Pb-Fe ($r = 0.301$, std. Dev. = 0.112). (Figure 13, Appendix II). Correlation of lead with Mn, Cd, Mg and K is low with lowest significant level. Furthermore, Correlations between Pb-Cd, Pb-S, Pb-Zn and Pb-Si are relatively less fluctuable (Figure 13) whereas in the case of Pb-Mg and Pb-K it is highly deflected. The different level of adsorption and variance is the result of the ambient concentration of metals, relative affinities for available surface sites, and possible kinetics as these are the governing factors for adsorption of metal ions [Coughlin and Stone, 1995]. The mean correlation with Mn ($r=0.232$) compare to Fe($r=0.301$) and S($r=0.319$) indicates that lead prefers to follow and adsorb with later elements than Mn. Moreover, higher deviation values for Mn (0.139) compare to Fe (0.112) and S (0.102) also indicate the competition between elemental binding sites. Mg has shown greater affinity towards the Mn with high binding coefficients ($r=0.41$) and low deviation (0.169) values compare to Fe ($r= 0.307$ and std. dev.= 0.178). There might be a competition between metals like Pb and Mg for sharing the binding sites at Fe and Mn. Beside that the significant correlation on most of the particles with Pb could be due the association of it with iron which is finally associated with Si. The lowest variation of Zn (0.079) with Pb could be interpreted as both of them are sharing the same bonding sites in the particles.

Competition with other elements, speciation of Fe on the sediment surface, the speciation of Pb in water and surface site activity plays significant role in binding of Pb to sediment particles. [Rauch and Morrison, 2003]. Rauch and Morrison (2003) in a similar speciation work have reported low level of Pb in relative to occurrence of Mg on the same sample. Mg is found to be abundant and may primarily fill adsorption sites on Fe. Correlation coefficient of Pb with Cd and K is very low i.e. 0.22 and 0.145 with deviation 0.06 and 0.20 respectively. In the case of Pb-Mg, the variability and the binding coefficient reveals that there is competition in some particles for the same binding site between them. In the case of Pb-Cd, lower variability may be the reason of forming fairly stable compounds with the available site on the particles after binding of other elements. High correlation coefficients observed on the case of combination of Cd, K and Zn with Si compare to Mg and Pb is the result of these combinations shifting to other combination sites than of Pb.

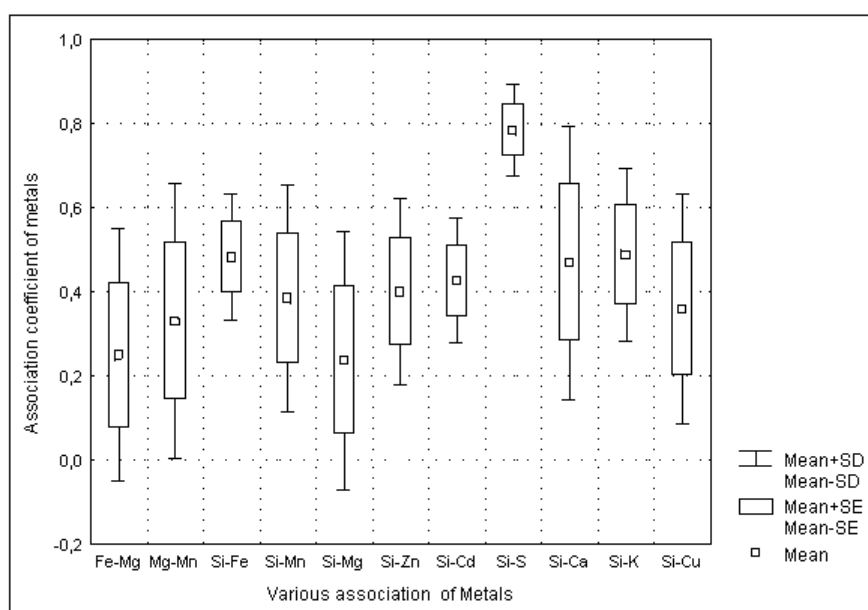


Figure 14: Diagram showing mean correlation coefficients and variability between different elements.

Notwithstanding, among the elements, correlation of Mg with Si is comparatively weaker with high variability (Figure 14, Appendix II) in compare to the correlation of same elements with Mn. It may be that Mg favours the binding site of Mn rather than Si. Beside that, comparing the association of Mg with Fe and Si, it can be seen that coefficient of binding is almost similar where as the variation is higher in the case of Si than with Fe. Looking on each particle it can be seen that the binding coefficient in each particle is opposite to each other i.e. increasing and decreasing. It can be say that after binding with Mn, Mg favours the association with either Si or Fe.

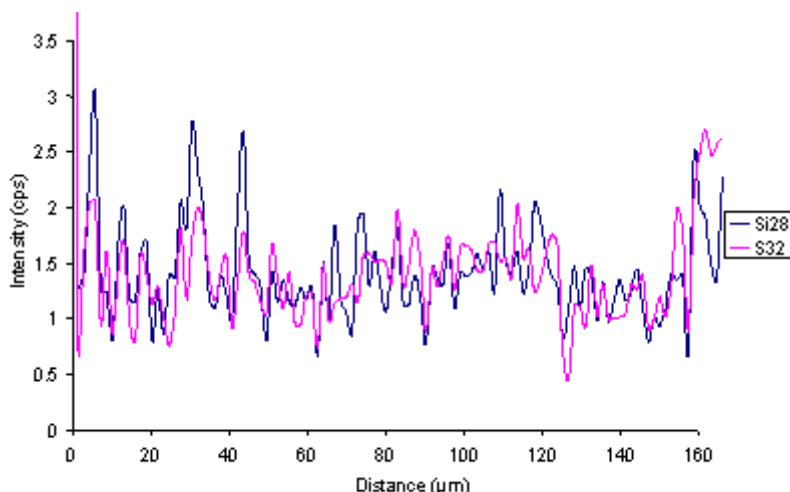


Figure 15: Normalized profile of Si and S across the surface of a sediment particle.

Correlation between Si and S is found to be stronger followed by Si-Ca and Si-Fe (Figure 14). Beside the correlation coefficients, the normalized signal (Figure 15) also shows a good correlation between Si and S with the occurrence of Si peak with S peak in many instances. Lower variability measured in the case of Si-S indicates that the S prefers to form bonding with Si than later two elements. In the case of Ca and S, Ca has comparatively higher variation than Fe while bonding with Si. On the other hand, the correlation coefficient between Ca-S is higher with comparatively higher variation than Fe-S. Moreover, the correlation between Ca-Fe is found to be weaker than both of these values. There may be competition between Ca, S and Fe for sharing the bonding site with Si. From the relation between Ca and Fe it can be said that it may have filled the binding sites with iron after filling the sites of Si and S. Notwithstanding, as Fe, S and Ca have competed for the binding site with Si, the weak correlation seen between Fe and Ca may be the result of association within the previous elements. The major portion of the total Fe content is reported to be associated in the lattice structure of clay and silicate minerals because of the strong relation between Al and Fe. [Marin and Giresse, 2001]. Furthermore, major portion of iron is found to be present as sulphide and oxyhydroxides at oxic sediment sites [Kiratli and Ergin, 1996]. Association of Mn with Si is also observed in the particles ranging from 0.11 to 0.65 coefficients value with the variance level of 0.15. In most cases, strong correlation is observed indicating affections for the binding sites with Si. Bilali et al, 2002 has found competition of Mn with residual carbonate compounds, silicates as well as Fe and Mn oxides in different oxic sediment samples. Because of Strong association of S, Ca, Fe with Si it is also possible for Mn to have significant correlation combining with these elements. Furthermore, carbonate phases is found to hold significant amount of Mn and Pb [Kiratli and Ergin, 1996].

In the case of Cu it is found that its correlation with Pb is relatively lower than with Si. Whereas, the correlation is highly variable in the case of Cu-Si than in Cu-Pb as well as the significant correlation level is also greater. Weaker correlation coefficients with Pb are the indication of preference of Cu to different binding site than Pb. As the significant

level is higher in the case with Si, there may be association of Cu directly with Si or with other elements like metallic sulphur or Fe/Mn oxides. Rauret et al., (1988) have reported higher percentage of Cu bonded to residual fraction and much lower contents are associated to carbonates and Fe/Mn oxides [Rauret et al., 1988].

6.2.2 Degree of association

In order to calculate percentage association or degree of association of elements, elemental peaks are identified based on peak greater than or equal to twice of its base signal. Peaks occurring simultaneously are then expressed as percentage/degree of association. Two elements are considered to be associated if signal peaks occur at the same place for both elements.

Particles	Percentage association of Pb to			
	Fe	Mn	Fe, Mn	Ca
1	75	50	42	67
2	72	77	64	55
3	53	59	35	47
4	54	48	30	32
5	58	61	48	35
6	75	65	47	36
7	55	69	47	44
8	55	40	35	45
9	61	48	39	45
10	55	51	45	48
11	44	60	34	25
12	50	57	36	42
Average %	59%	57%	42%	43%

Table 2: Degree of association of Pb to different elements like Fe, Mn and Ca expressed as the percentage of association of elemental peaks.

The average degree of association of Pb to Fe and Mn is 59% and 57% respectively (Table 2). Furthermore, degree of association is 42% for Pb coinciding to Fe and Mn at same peak point. On calculation from above values, degree of association of Pb to Fe and/or Mn is 72%. This is an indication that lead is associated with one of the geochemical phases of Fe/Mn oxides. Ca is considered as an indicator for the association of Pb to carbonates. 43% of Pb's signal intensity/peaks are occurred with Ca peaks. This is probably an indication that carbonates groups are second to Fe/Mn oxides for adsorption of Pb. Tasai et al. 1998, has reported most of the Pb associated with Fe oxides and Carbonates on river sediments [Tasai et al., 1998]. Higher percentage of Pb is found to be associated with Fe/Mn oxides on river sediments [Rauret et al., 1988]. Relatively weaker correlation observed before between Pb and other different elements may be due to the signal values other than intense signal peaks. It could be possible to observe good

correlation in harmony with degree of association if only the peaks of these elements are considered for correlation.

In the above Table 2, sum of association is greater than 100%. The reason for this is that the resolution obtained for different elements on LA-ICP-MS have mixed phases of different bulk and trace elements, e.g. Fe oxides and Carbonates. The mixed phase of different elemental signals can be seen from the following Figure 15 as well.

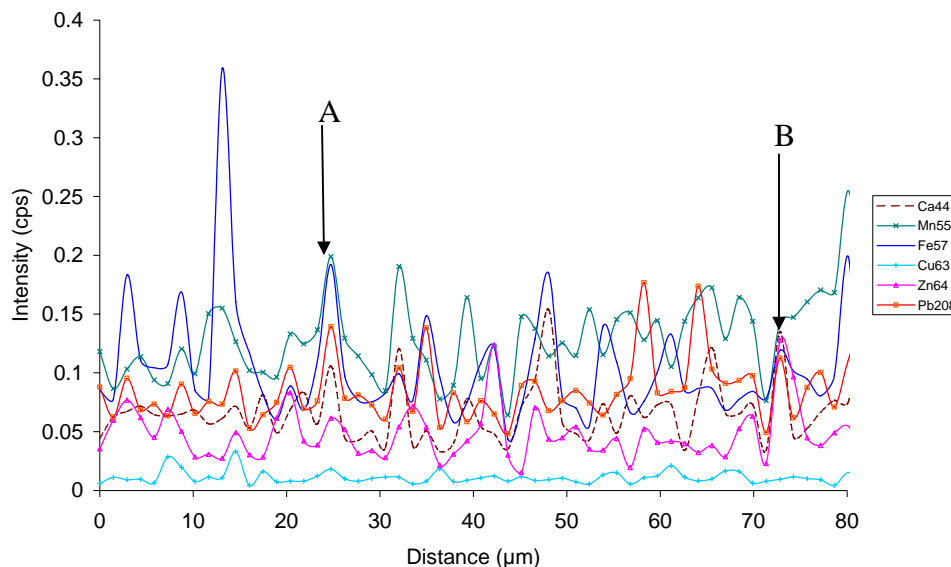


Figure 16: Normalized profile of different elements across the surface of a sediment particle.

The competition between the elements could be observed from the normalized signal between different elements present in Figure 16. In the Figure 15 point A represents a site where all five elements: Ca, Mn, Fe, Cu, Zn and Pb have peak intensity at the same spot of the particle. All these elements following Fe and Mn in this case could be the result of association of these elements with Fe and Mn or only with one of them i.e. Fe or Mn. However, it may be an indication that all these elements on this spot of the particles suggesting as they are sharing the same binding site like Fe, Mn and S which is finally adsorbed or bonded to Aluminium silicate. Similarly, in the point B, it could be observed that only the intensity of Cu is not so distinct whereas the intensity of Zn is high in compare to point A. Beside that the intensity of Fe and Mn has also decreased. It could be an indication that on this point of the particle-binding site for other elements are not so favourable and the competition resulted in the high intensity of Zn and Ca. However, the good correlation could be observed for some elements on the signal intensity profile obtained by LA-ICP-MS, there could be some restrictions on observing the correlation between the elements due to the different peak intensity observed on the particle profiles, for e.g. Cu with other elements (Figure 16).

6.2.3 Ternary plots and three-dimensional diagrams

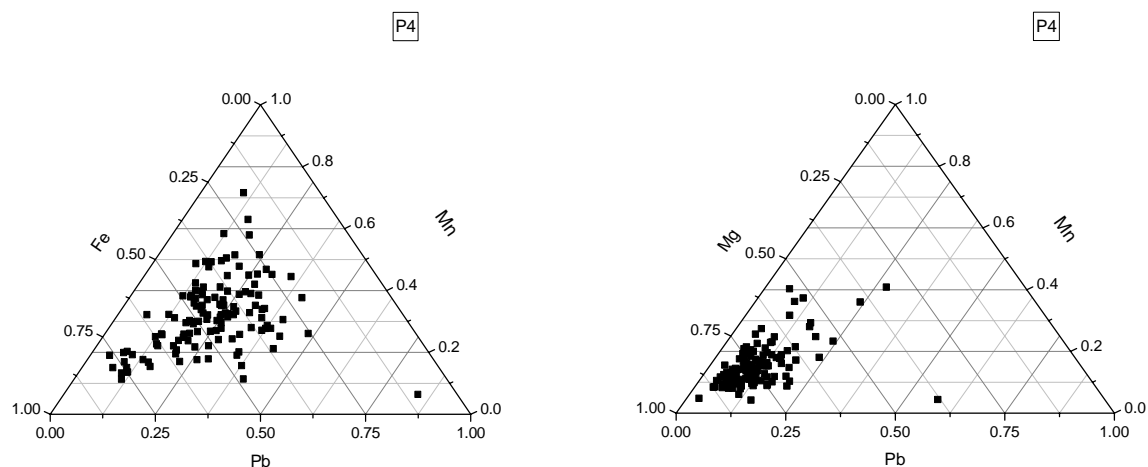


Figure 17: Figures showing the relationships between Pb/Mn/Fe and Pb/Mn/Mg

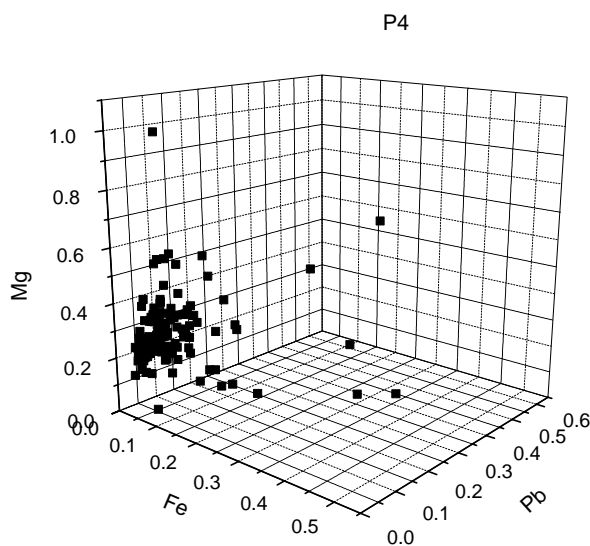


Figure 18: Three-dimensional relationship for the signal intensities between Fe, Mg and Pb.

Since correlation shows the consistency of elements within particles, it doesn't always tell about the relative richness of the elements. Lower correlation level observed in most of the elements, however they are significant at lower level, indicates that the correlation between two variables is not only due to themselves. Third variance or elements

underlying on the particle is affecting themselves. In viewing this, a good idea is to look for richness of the elemental ratio, which is also possible through ternary diagram. The ternary diagrams represent ratio percentage of three different elements on three-dimensional way. In Figure 17 (Pb/Mn/Fe), cluster of values are relatively deviated towards iron. It can be said that the richness of Pb with Fe is relatively higher than Pb with Mn. In the case of Pb/Mn/Mg, richness of Mg is higher with Mn compare to Pb with Mn. Beside that three-dimensional diagram (Figure 18) for the same particle (P4) also shows that Pb has few intense peaks with Fe. On other elements also Pb and Fe has shown few intense ratio peaks (Figure 20, Appendix III). However, in most cases relationship between elemental signal values between Mg and Fe is stronger. This could be possibly due the competition between Mg and Pb to the adsorbing site of Fe and whenever favours Pb forms intense peaks with Fe.

Descriptions and figures presented above could support an idea of aluminium silicate being a core of particles. It could be possible that the particles with aluminium silicate core have the coatings of Fe/Mn oxides and S on it where other metals are also competing for the bonding sites. In the oxic sediments association of trace metals with HS coatings on various types of particles could dominant metal binding [Tessier et al., 1996]. Fe/Mn oxides were identified as active support materials for the adsorption of metals like Pb and Zn [Barauh et al., 1996; Jain and Ram, 1997]. However, the correlation always doesn't tell us about the practical correlation or association on the sediment particles. Metals might be adsorbed on other elements, which finally was sorbed to silicate particles. Manganese oxides (MnOx), iron hydrous oxides (FeOx), reactive particulate organic carbon are the main sediment component that influences the adsorption of metals on the sediments [Shea, 1988]. Moreover, the precipitation of metal sulphides (MeS) may also control the distribution of metal between the aqueous and sediment phase. Some of the iron oxides commonly found are ferrihydrite, hematite, magnetite, goethite, lepidocrite and feroxyhite [Trivedi et al, 2001]. Based on the correlation and ternary diagrams it can be said that Fe/Mn oxides are a significant adsorbents of Pb and Mg on the sediments from Mölndal River.

7 Conclusion

Sequential extraction has been used for most of the speciation analysis. However, advancement in LA-ICP-MS has assisted in study of elemental speciation or associations at micrometric scale keeping the heterogeneity of the particles. While looking at the ablated particle it has been realized that within the same sediment particles also different elements within different particles have different ablation behaviour. This was the reason that out of 50 particles ablated only few were able to be used for the further analysis. Statistical analysis like autocorrelation has shown that elemental profiles of all elements on time series are not independent. This is an indication that with the same energy of ablation, the richness of the elements on the particles and softness/hardness within the particles affect the elemental profiles and the intensity of peaks. It is thus suggested that any further study dealing with quantification of peak intensity and optimisation of the laser parameters for different elements should incorporate this test.

Based on the correlation analysis, degree of association and ternary/three dimensional plots, Fe/Mn oxides are found to be the main adsorption sites for many trace elements. Pb is found to be associated with Fe fraction rather than on Mn fraction. Moreover, degree of association has shown that Fe and/or Mn oxides are one of the favourable bonding sites for Pb. Ca, as an indicator of carbonate groups has also shown good degree of association (43%) to Pb. Competition between Pb and Mg is observed and Mg is found to favour association with Fe. Three-dimensional ternary diagram has also suggested relative richness of Mg with Mn rather than with Fe. However, three-dimensional diagram between Fe, Pb and Mg has shown few intense peaks of Pb to Fe. This suggests that whenever the condition favours Pb binds with Fe. This analysis has supported an idea of aluminium silicate as a core of the sediment as most of the elements have good correlation with it. Higher variance observed in the case of Pb with Ca/K indicates that the competition between the elements on the particle affects the association and richness of elements. Based on this study it is most likely that the particle has coating of Fe/Mn oxides and S compounds on the sediment where the adsorption of other elements in competitive complex form occurred.

Acknowledgement

I would like to thank time for his assistance through Chalmers University of Technology and The Swedish Institute, Sweden.

All you people out there-teachers and friends who are also a part of time are also acknowledged for friendly discussions, suggestions occurred during my stay at Sweden.

I don't miss the opportunity to thank my supervisor Dr. Sebastien Rauch and Examiner Prof. Greg Morrison for their inexhaustible support, encouragement, scientific advice and insights. Hope I was able to carry out a good work. Sharon Kuhlmann! Your advice and suggestion are also unforgettable.

Family members and others: "non-named", "non-forgotten" out there are also constant source of my inspiration.

References

- Alexander**, M. L.; Smit, M.R.; Hartman, J.S.; Mendoza, A.; Koppenaal, D.W.; *Applied Surface science*, **1998**, 127-129, 255-261.
- Ariza**, G. J. L.; Giraldez, I.; Sanchez-Rodas, D.; Morales, E.; *Talanta*, **2000**, 52, 545-554.
- Arrowsmith**, P.; *Analytical Chemistry*; **1987**, Vol. 59, 1437-1444.
- Baruah**, N. K., Kotoky, P., Bhattacharyya, K. G., Borah, G. C.; *The Science of Total the Environment*; **1996**, Vol. 193, 1-12.
- Beauchemin**, D.; *Current status of ICP-MS in Comprehensive Analytical Chemistry*; Ed. Barcelo, D., 2000, Volume XXXIV, Elsevier.
- Bermond**, A; *Analytica Chimica Acta*, **2001**, 445, 79-88
- Bewers**, J. M.; Barry, P. J.; MacGregor, D. J.; *Distribution and Cycling of Cadmium in the Environment in Cadmium in the Aquatic Environment*; Ed. By Nriagu, J. O.; Sprague, J. B., **1987**, Volume 19, A Willey- Interscience Publication.
- Bilali**, L. E.; Rasmussen, P. E.; Hall, G. E. M.; Fortin, D.; *Applied Geochemistry*, **2002**, 17, 1171-1181.
- Bloom**, P. R., and Erich, M. S.; *The Quantitation of Aqueous Aluminum in The Environmental Chemistry of Aluminum*, Ed. Sposotio, G., **1996**, Second Edition, Lewis Publishers, CRC Press.
- Bordas**, F., and Bourg, A. C. M.; *Water, Air, and Soil Pollution*, **1998**, 103: 137-149.
- Coughlin**, R. B., and Stone, T. Alan; *Environment Scinece and Technology*, **1995**, 29, 2445-2455.
- Das**, A. K.; Guardia, M., Cervera, L. M.; *Talanta*, **2001**, 55, 1-28.
- Davidson**, C. M.; Wilson, L. E.; Ure, A. M.; *Fresenius Journal of Anal. Chem.*, **1999**, 363: 134-136.
- Dawdy**, D.R, and Matalas, N.C.; *Statistical and probability analysis of hydrologic data, Part III: Analysis of variance, covariance and time series*, in Ven Te Chow, ed., *Handbook of applied hydrology, a compendium of water-resources technology*, **1964**, New York, McGraw-Hill book Company, p. 8.68-8.90.

Driscoll, C. T., and Postek, K. M.; *The Chemistry of Aluminum in Surface Waters in The Environmental Chemistry of Aluminum*, Ed. Sposotio, G., **1996**, Second Edition, Lewis Publishers, CRC Press.

Durrant, S. F.; *J. Anal. Atomic Spectrometry*, **1999**, 14, 1385-1403.

Fytianos, K.; *Journal of AOAC INTERNATIONAL*, **2001**, Vol. 84, No. 6.

Glazewski, R., and Morrison, G. M.; *The Science of the Total Environment*, **1996**, 189/190, 327-333.

Gleyzes, C.; Tellier, S.; Astruc, M.; *Trends in Analytical Chemistry*, **2002**, Vol. 21, No. 6+7.

Gunther, D.; Horn, I.; Hattendorf, B.; *Fresenius J. Anal. Chem.*, **2000**, 368: 4-14.

Gunther, D.; Jackson, S. E.; Longerich, H. P.; *Spectrochimica Acta Part B*, **1999**, 54, 381-409.

Gunther, D.; Mermet, J. M.; *Laser ablation for Inductively Coupled Plasma-Mass Spectrometry in Comprehensive Analytical Chemistry*; Ed. Barcelo, D., **2000**, Volume XXXIV, Elsevier.

Guo, T.; Delaune, R. D.; Patrik Jr, W. H.; *Environment International*, **1997**, Vol. 23, No. 3, pp. 305-316.

Izquierdo, C.; Usero, J.; Gracia, I.; *Marine Pollution Bulletin*, **1997**, Vol. 34, No. 2, pp. 123-128.

Jain, C. K., and Ram, D.; *Water Research*; **1997**, Vol. 31, No. 1, pp. 154-162.

Kheboian, C., and Bauer, C. F.; *Analytical chemistry*, **1987**, 59, 1417-1423.

Kiratli, N., and Ergin, M.; *Applied Geochemistry*, **1996**, Vol. 11, pp. 775-788.

Klemm, W., and Bombach, G.; *Fresenius Journal of Anal. Chem.*, **2001**, 370: 641-646.

Kot, A., and Namiesnik, J.; *Trends in Analytical Chemistry*, **2000**, Vol. 19, No. 2+3.

Li, X.; Shen, Z.; Wai, O. W. H.; Li, Y. S.; *Marine pollution Bulletin*, **2001**, Vol. 42, No. 3, pp. 215-223.

Lobinski, R.; *Spectrochimica Acta Part B*, **1998**, 53, 177-185.

Marin, B., and Giresse, P.; *Marine Geology*, **2001**, 172, 147-165.

Mester, Z.; Cremisini, C.; Ghiara, E.; Morabito, R.; *Analytica Chimica Acta*, **1998**, 359, 133-142.

Raksasataya, M.; Langdon, A. G.; Kim, N. D.; *Analytical Chimica Acta*, **1996**, 332, 1-14.

Rauch, S., and Morrison, G. M.; *Manuscript submitted to "The Science of the Total Environment"*, **2003**.

Rauch, S.; Morrison, G. M.; Motelica-Heino, M.; Donnard, O. F. X.; Muris, M.; *Environ. Sci. Technol.*, **2000**, 34, 3119-3123.

Rauch, S.; *On the Environmental Relevance of Platinum Group Elements*, **2001**, Thesis for the Degree of Doctor of Philosophy, Water Environment Transport, Chalmers University of Technology, Göteborg, Sweden.

Rauret, G.; Rubio, R.; Lopez-Sanchez, J. F.; Casassas, E.; *Water Research*, **1988**, Vol. 22, No. 4, pp. 449-455.

Rice, K. C.; *Environ. Sci. Technol.*, **1999**, 33, 2499-2504.

Shea, D.; *Environ. Sci. Technol.*, **1988**, Vol. 22, No.11, 1988.

Stone, M.; Droppo, I. G.; *Environmental Pollution*, **1996**, Vol. 93, No. 3, pp. 353-362.

Tam, N. F. Y., and Yao, M. W. Y.; *The Science of the Total Environment*, **1998**, 216, 33-39.

Tsai, L., J.; Yu, K., C.; Chang, J., S.; Ho, S., T.; *Water Science and Technology*; **1998**, Vol. 37, No. 6-7, pp. 217-224.

Tessier, A.; Campbell, P. G. C.; Bisson, M.; *Analytical Chemistry*, **1979**, Vol. 51, No. 7.

Tessier, A.; Fortin, D.; Belzile, N.; DeVitre, R. R.; Leppard, G. G.; *Geochimica et Cosmochimica Acta*, **1996**, Vol. 60, No.3, pp.387-404.

Trivedi, P.; Axe, L.; Dyer, J.; *Collids and Surfaces A: Physicochemical and Engineering Aspects*, **2001**,191, 107-121.

Walting, R. J.; Lynch, B. F.; Herring, D.; *Journal of Analytical Atomic Spectrometry*, February **1997**, Vol. 12, 195-203.

Walting, R. J; Herbert, H. K.;Barrow, I. S.; Thomas, A. G.; *Analyst*, May **1995**, Vol. 120, 1357-1364.

Webb, M. S.; Leppard, G. G.; Gaillard, F. J.; *Environ. Sci. Technol.*, **2000**, 34, 1926-1933.

Xue, H., and Sigg, L.; *Analytica Chimica Acta*, **1998**, 363, 249- 259.

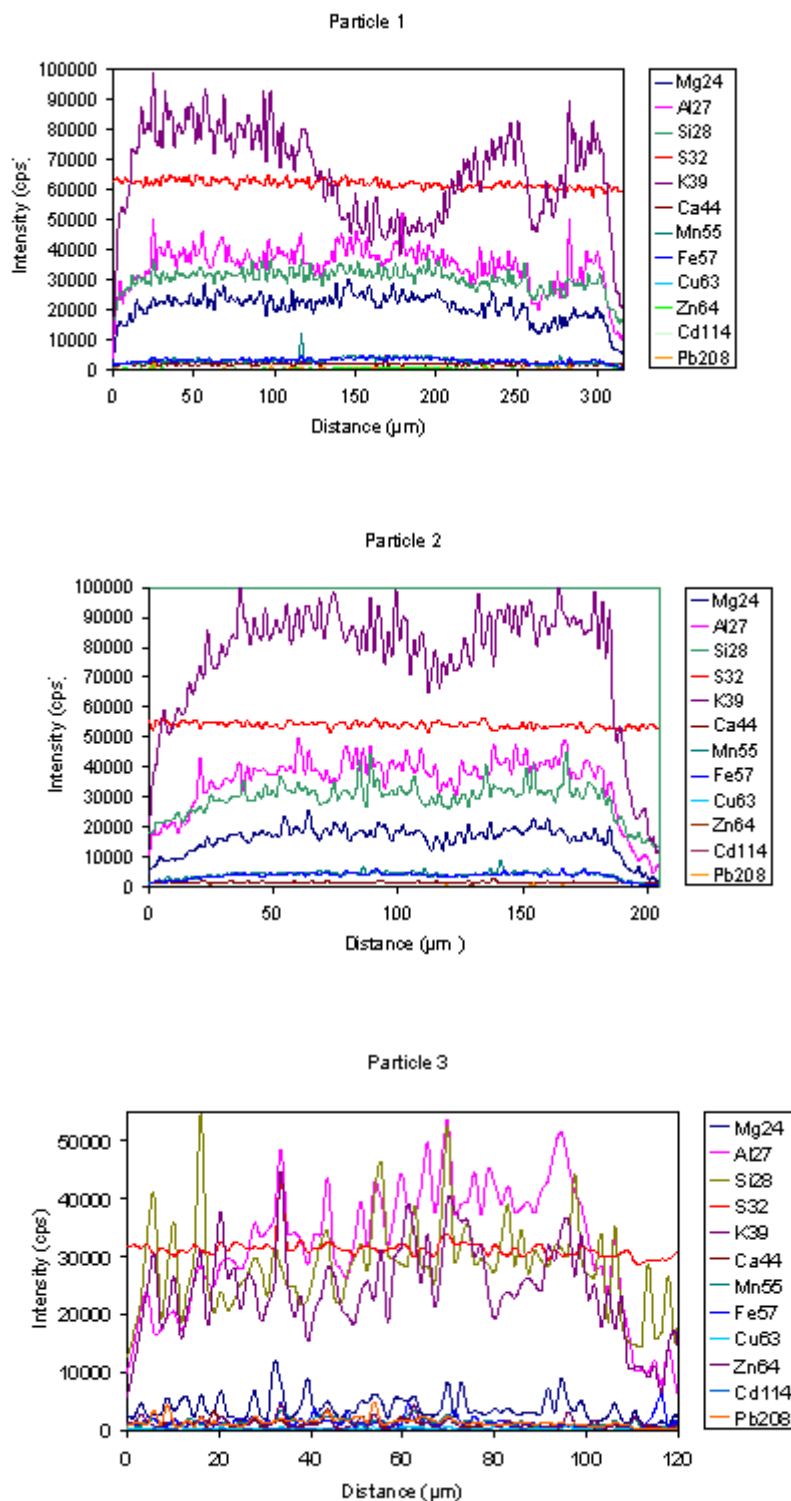
Yousfi, I., and Bermond, A.; *Environmental Technology*, **1997**, 18, 139

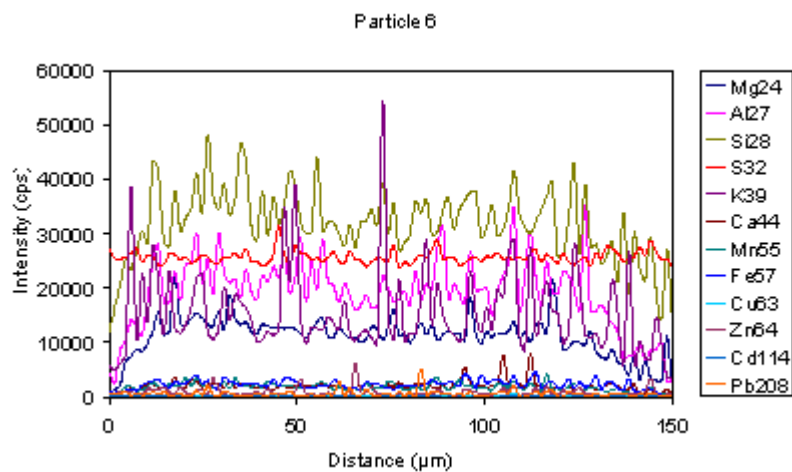
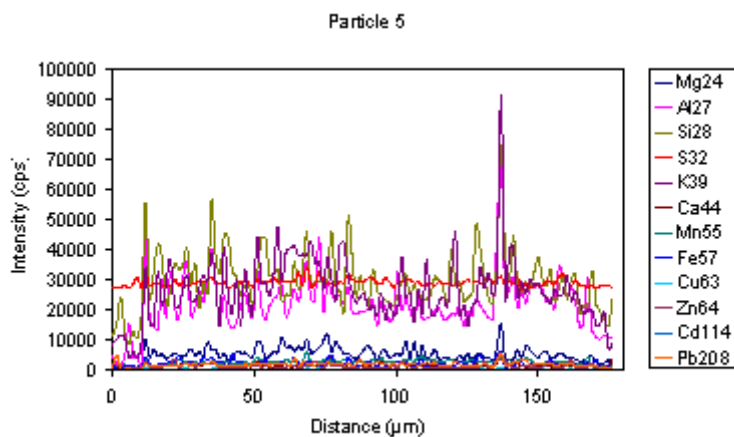
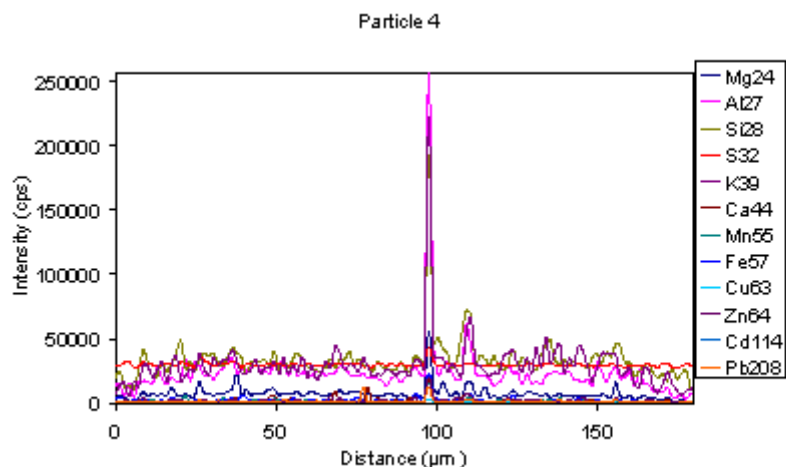
Yu, K. C.; Tsai, L. J.; Chen, S. H.; Ho, S. T.; *Water Research*, **2001**, Vol. 35, No. 10, pp. 2417-2428.

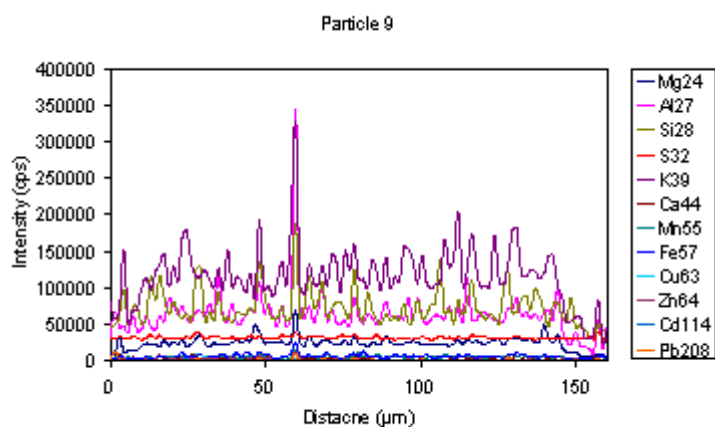
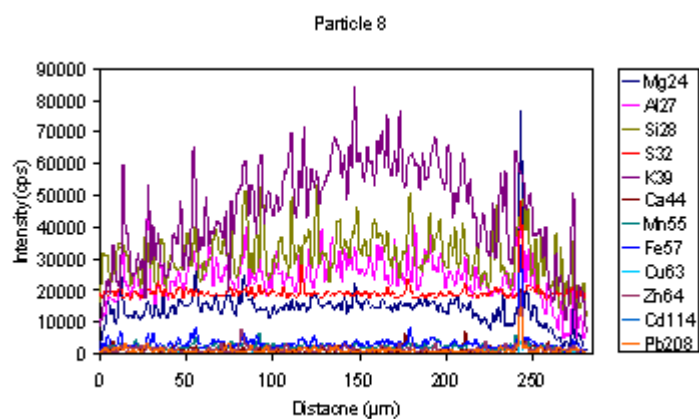
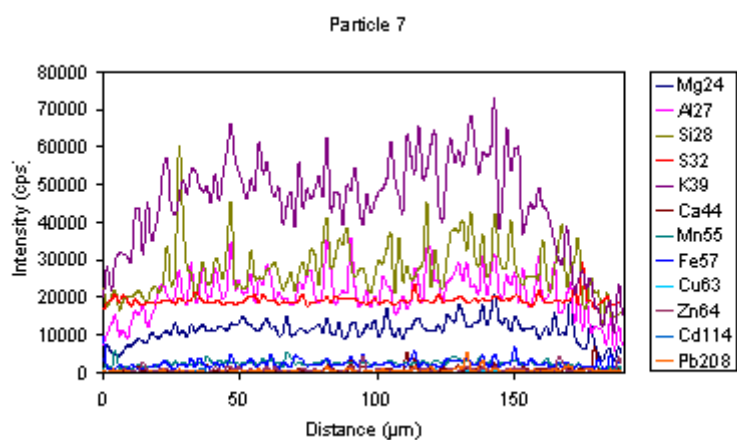
Zoorob, G. K.; Mckiernan, J. W.; Caruso, J. A.; *Microchimica Acta*, **1998**, 128, 145-168.

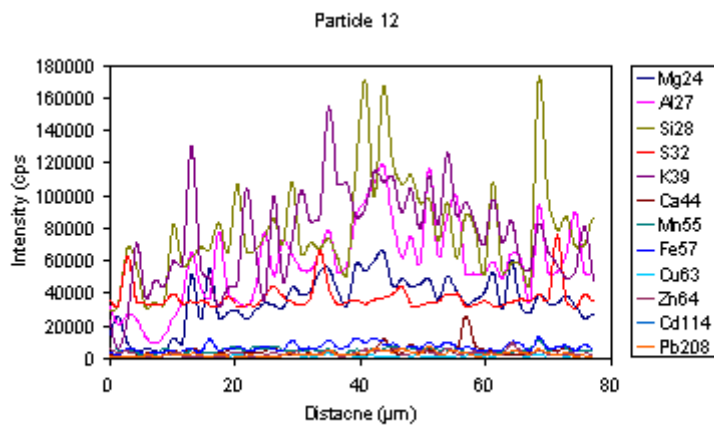
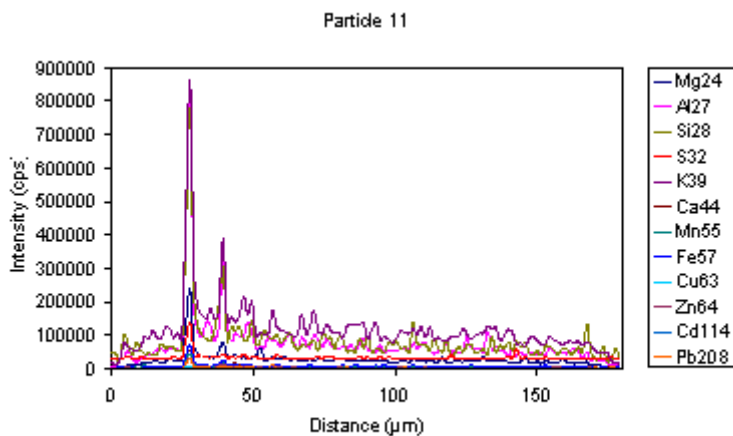
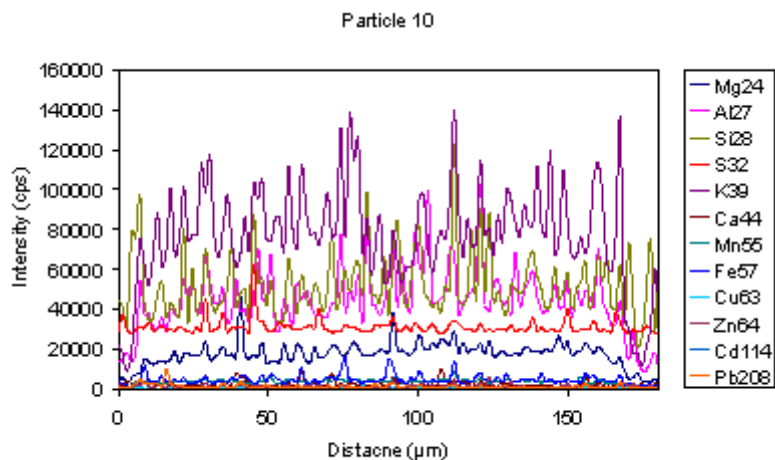
Appendix I

Figure 19: Elemental profiles of different element on different particles used on this analytical work.









Appendix II

(Note: * represents the significant correlation coefficients)

Table 3: Correlation between Pb-Mn and Pb-Fe

Particles	r (Pb-Mn)	Significances	r (Pb-Fe)	Significances
1	0.09238	-	0.16255	-
2	0.04425	-	0.18038	-
3	0.44118	*	0.23472	-
4	0.36022	*	0.26124	-
5	0.43458	*	0.22053	-
6	0.29986	*	0.43744	*
7	0.11021	-	0.37692	*
8	0.31493	*	0.38593	*
9	0.17879	-	0.33178	*
10	0.13545	-	0.38251	*
11	0.15742	-	0.48705	*
12	0.21741	-	0.16216	-
Mean	0.23222		0.30193	
Std. Dev.	0.13492		0.11251	

Table 4: Correlation between Pb-Cu and Pb-Zn

Particles	r (Pb-Cu)	Significances	r (Pb-Zn)	Significances
1	0.14384	-	0.25361	-
2	NA	-	0.38596	*
3	0.17028	-	0.36721	*
4	0.26048	-	0.27881	*
5	0.26650	-	0.26723	-
6	0.31540	*	0.35452	*
7	0.25083	-	0.25083	-
8	0.46321	*	0.19642	-
9	0.36853	*	0.43727	*
10	0.21979	-	0.30491	*
11	0.52597	*	0.45230	*
12	0.19202	-	0.36705	*
Mean	0.28880		0.32635	
Std. Dev.	0.12069		0.07973	

Table 5: Correlation between Pb-Cd and Pb-Mg

Particles	r (Pb-Cd)	Significances	r (Pb-Mg)	Significances
1	0.15308	-	-0.0461	-
2	0.25163	-	0.11211	-
3	0.22972	-	0.43146	*
4	0.13310	-	0.28888	*
5	0.21512	-	0.56503	*
6	0.15720	-	0.06310	-
7	0.16757	-	0.10347	-
8	0.29650	*	0.08175	-
9	0.21528	-	-0.0546	-
10	0.34319	*	0.08974	-
11	0.33094	*	0.26109	-
12	0.22071	-	-0.15450	-
Mean	0.22617		0.14512	
Std. Dev.	0.06924		0.20786	

Table 6: Correlation between Pb-Ca and Pb-S

Particles	r (Pb-Ca)	Significances	r (Pb-S)	Significances
1	0.33454	*	0.23782	-
2	NA		NA	
3	0.55485	*	0.16012	-
4	0.03106	-	0.20398	-
5	0.36743	*	0.32731	*
6	0.22963	-	0.43047	*
7	0.30114	*	NA	
8	0.43255	*	NA	
9	0.37804	*	0.41165	*
10	0.43348	*	0.43749	*
11	0.46465	*	0.37170	*
12	0.09873	-	0.29804	*
Mean	0.32965		0.31984	
Std. Dev.	0.15729		0.1021	

Table 7: Correlation between Pb-Si and Pb-K

Particles	r (Pb-Si)	Significances	r (Pb-K)	Significances
1	0.23520	-	NA	
2	NA		0.17186	-
3	0.19170	-	0.17480	-
4	0.32288	*	0.33070	*
5	0.46848	*	0.59756	*
6	0.44868	*	0.39822	*
7	0.20580	-	-0.1119	-
8	0.42185	*	0.03511	-
9	0.38086	*	0.18695	-
10	0.41094	*	0.09146	-
11	0.42502	*	0.24971	-
12	0.22002	-	0.33057	*
Mean	0.33922		0.22318	
Std. Dev.	0.10706		0.19128	

Table 8: Correlation between Ca-S and Fe-S

Particles	r (Ca-S)	Significances	r (Fe-S)	Significances
1	0.64602	*	0.41623	*
2	NA		NA	
3	0.49721	*	0.53251	*
4	0.30085	*	0.33214	*
5	0.66721	*	0.55479	*
6	0.47302	*	0.43625	*
7	NA		NA	
8	NA		NA	
9	0.62066	*	0.51686	*
10	0.60134	*	0.28647	*
11	0.41580	*	0.50976	*
12	0.52842	*	0.58696	*
Mean	0.52784		0.46355	
Std. Dev.	0.12012		0.10302	

Table 9: Correlation between Fe-Ca and Fe-Mg

Particles	r (Fe-Ca)	Significances	r (Fe-Mg)	Significances
1	0.42539	*	0.26793	-
2	NA		0.49585	*
3	0.60592	*	0.20633	-
4	0.23413	-	0.28125	*
5	0.46265	*	0.29311	*
6	0.47185	*	0.29280	*
7	0.14946	-	0.07124	-
8	0.24791	-	0.51712	*
9	0.32891	*	0.45990	*
10	0.21832	-	0.44647	*
11	0.52475	*	0.42949	*
12	0.30351	*	-0.0735	-
Mean	0.36116		0.30733	
Std. Dev.	0.14557		0.17857	

Table 10: Correlation between Mg-Mn and Si-Fe

Particles	r (Mg-Mn)	Significances	r (Si-Fe)	Significances
1	0.36840	*	0.53049	*
2	0.49200	*	NA	
3	0.43597	*	0.48385	*
4	0.26176	-	0.33781	*
5	0.42719	*	0.58063	*
6	0.43576	*	0.49670	*
7	0.45956	*	0.37798	*
8	0.34708	*	0.38563	*
9	0.60961	*	0.46903	*
10	0.55671	*	0.34087	*
11	0.56401	*	0.55100	*
12	-0.0289	-	0.63732	*
Mean	0.41077		0.47194	
Std. Dev.	0.16953		0.10053	

Table 11: Correlation between Si-Mn and Si-Mg

Particles	r (Si-Mn)	Significances	r (Si-Mg)	Significances
1	0.11343	-	0.27339	*
2	NA		NA	
3	0.35984	*	0.40096	*
4	0.31695	*	0.30578	*
5	0.45272	*	0.42723	*
6	0.53408	*	0.48266	*
7	0.40003	*	0.36277	*
8	0.41456	*	0.16685	-
9	0.36976	*	0.45811	*
10	0.15496	-	0.09875	-
11	0.52705	*	0.24900	-
12	0.65271	*	-0.0976	-
Mean	0.39055		0.30762	
Std. Dev.	0.15861		0.18631	

Table 12: Correlation between Si-Zn and Si-Cd

Particles	r (Si-Zn)	Significances	r (Si-Cd)	Significances
1	0.27944	*	0.27451	*
2	NA		NA	
3	0.51699	*	0.45972	*
4	0.44394	*	0.38526	*
5	0.60662	*	0.57026	*
6	0.49687	*	0.54579	*
7	0.28902	*	0.27252	*
8	0.16645	-	0.42555	*
9	0.41880	*	0.33834	*
10	0.50142	*	0.56204	*
11	0.55897	*	0.50338	*
12	0.43717	*	0.49554	*
Mean	0.42870		0.43935	
Std. Dev.	0.13316		0.10932	

Table 13: Correlation between Si-S and Si-Ca

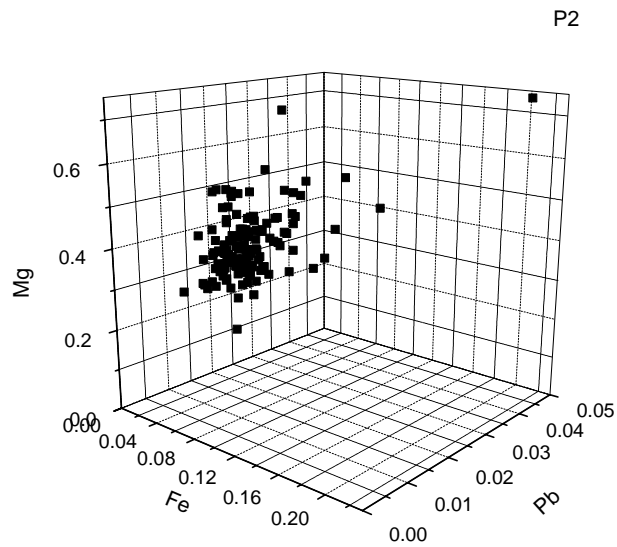
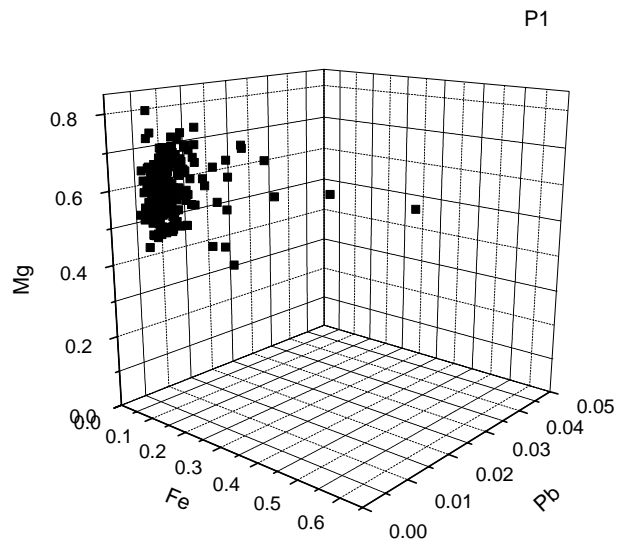
Particles	r (Si-S)	Significances	r (Si-Ca)	Significances
1	0.88798	*	0.77966	*
2	NA		NA	
3	0.82264	*	0.47953	*
4	0.75997	*	0.31739	*
5	0.82469	*	0.70916	*
6	0.88995	*	0.52693	*
7	NA		0.13106	-
8	NA		0.31332	*
9	0.72829	*	0.55205	*
10	0.81009	*	0.56495	*
11	0.71317	*	0.53473	*
12	0.67258	*	0.59132	*
Mean	0.78993		0.50001	
Std. Dev.	0.07637		0.18544	

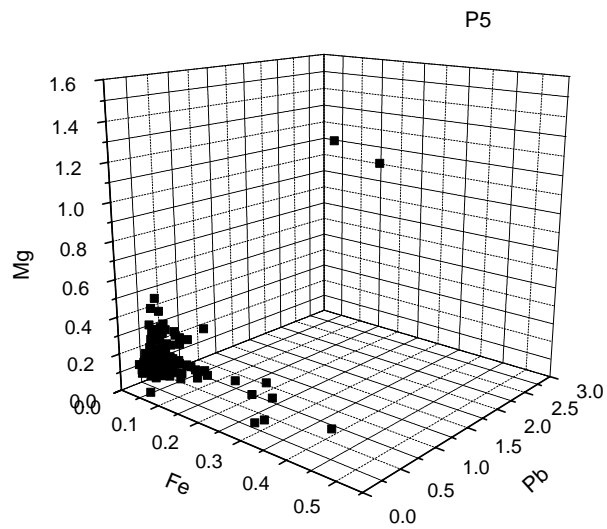
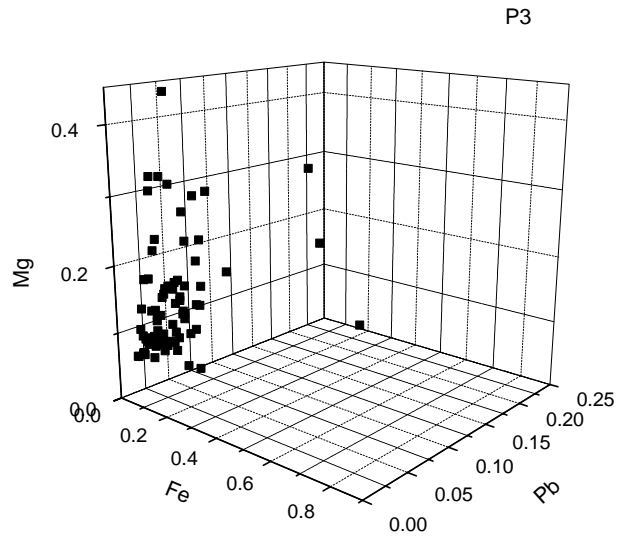
Table 14: Correlation between Si-K and Si-Cu

Particles	r (Si-K)	Significances	r (Si-Cu)	Significances
1	NA		0.29424	*
2	NA		NA	
3	0.63609	*	0.43627	*
4	0.58555	*	0.17973	-
5	0.70406	*	0.63278	*
6	0.43142	*	0.46737	*
7	0.29259	*	0.08461	-
8	0.30537	*	0.29469	*
9	0.61448	*	0.25838	-
10	0.30797	*	0.39394	*
11	0.34386	*	0.60409	*
12	0.47206	*	0.36210	*
Mean	0.46935		0.36438	
Std. Dev.	0.15593		0.16719	

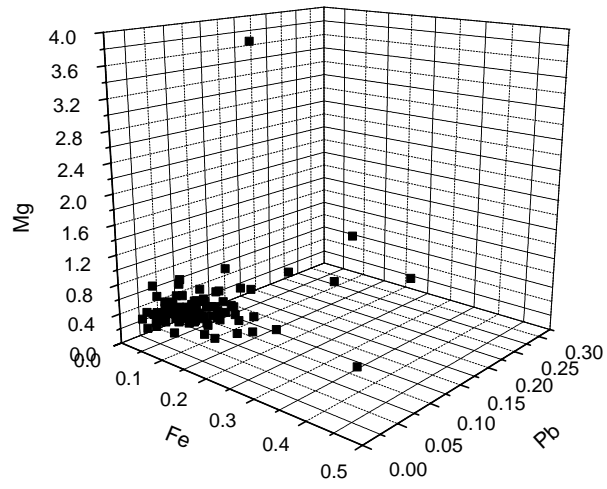
Appendix III

Figure 20: Three-dimensional diagram showing the relationship between Fe, Pb and Mg.

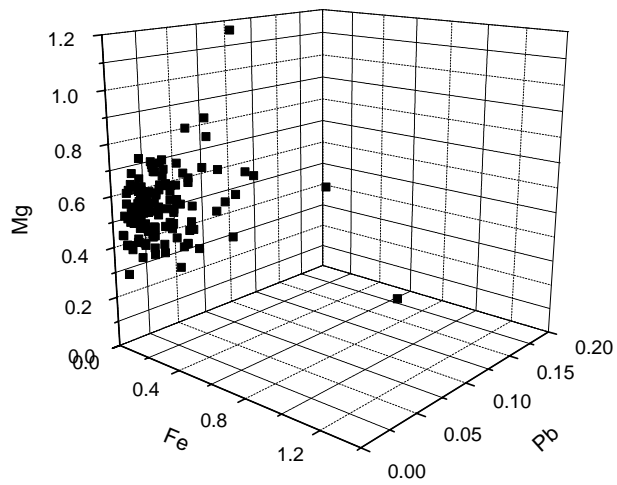


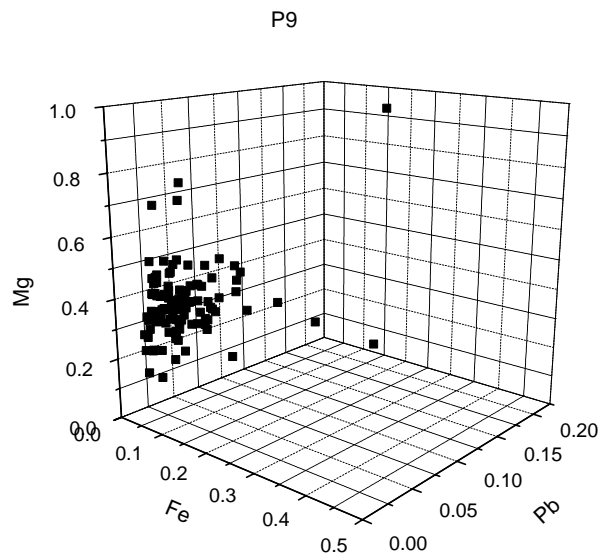
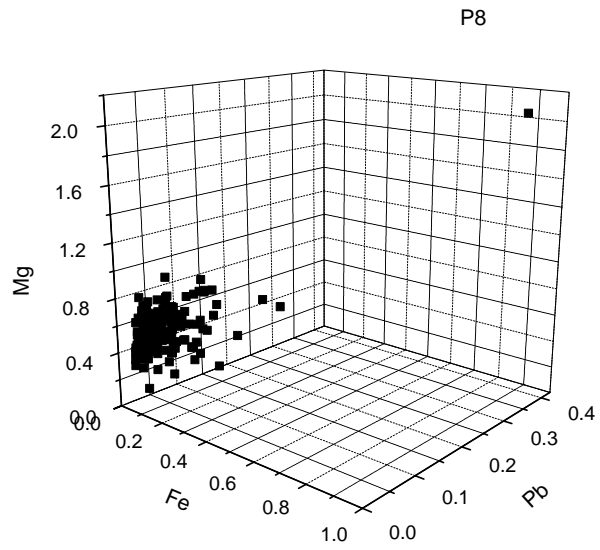


P6

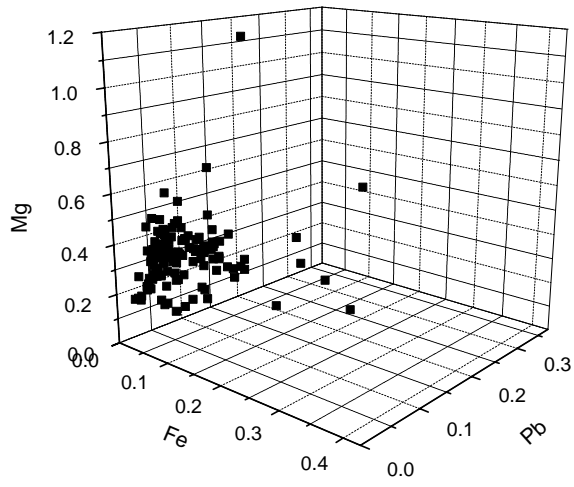


P7





P10



P11

